Published December 18, 2006

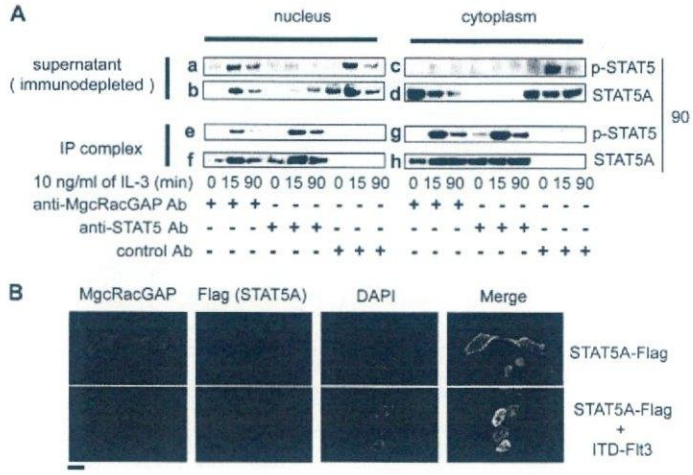

Figure 2. **STAT5A and MgcRacGAP simultaneously entered the nucleus.** (A) Stoichiometry of the association between MgcRacGAP and p-STAT5A or total STAT5A in the cytoplasm and nucleus. IL-3–starved Ba/F3 cells were stimulated with IL-3 for the times indicated, and cytosol and nuclear extracts were prepared as described previously (Nakamura et al., 2002). 10 μg of protein for each of the extracts was immunodepleted with the anti-MgcRacGAP, anti-STAT5A, or control antibody, followed by immunoblotting with the anti–p-STAT5 and anti-STAT5A antibodies (a–d). The immunoprecipitates were also examined by Western blotting with the anti–p-STAT5 and anti-STAT5 antibodies (e–h). (B) STAT5A and MgcRacGAP translocated into the nucleus upon ITD-Flt3 stimulation in 293T cells. Cells were transfected with pME/STAT5A-Flag together with pMKIT (MOCK; top) or pMKIT/ITD-Flt3 (bottom). After 36 h, cells were immunostained with the anti-MgcRacGAP and anti-Flag antibodies and viewed using a Fluoview FV300 confocal microscope. Bar, 10 μm.

and colocalization of STAT5A and MgcRacGAP in the nucleus (Fig. 2 B). These results indicated that MgcRacGAP translocated to the nucleus concurrently with STAT5A in response to IL-3 and ITD-Flt3 stimulation. Intriguingly, a dominant-negative form of Rac1, N17Rac1, completely inhibited the ITD-Flt3–induced nuclear translocation of STAT5A (Fig. S2, available at http://www.jcb.org/cgi/content/full/jcb.200604073/DC1). This result suggested that the GTP-bound form of Rac1 was required for the nuclear accumulation of activated STAT5A. However, N17Rac1 was recently reported to inhibit not only Rac1 but also other Rho-GTPases (Debreceni et al., 2004). To confirm that the N17Rac1 inhibition of nuclear translocation of p-STAT5A was indeed due to the inhibition of Rac1, we used mouse embryonic fibroblasts derived from gene-targeted conditional Rac1-flox mice in the Rac2-null background (Gu et al., 2003).

Rac1 is required for the nuclear translocation of p-STAT5A in mouse embryonic fibroblast cells

ITD-Flt3 induced the nuclear localization of STAT5A-Flag in the presence of Rac1 (Fig. 3 A, a and b). However, when Rac1 was depleted by Cre recombinase in $Rac2^{-/-}Rac1^{flox/flox}$ fibroblasts (Fig. 3 B), the nuclear translocation of STAT5A was severely impaired (Fig. 3 A, c and d), and even p-STAT5 mostly remained in the cytoplasm (Fig. 3 A, e and f). In addition, CA-STAT5A did not enter the nucleus in the absence of Rac1 (unpublished data). We performed a similar analysis using $Rac1^{flox/flox}Rac2^{wt/wt}$ fibroblasts and obtained identical results. These results demonstrate that Rac1 plays an essential role in the nuclear translocation of p-STAT5A.

Rac1 and MgcRacGAP were required for the nuclear accumulation and transcriptional activation of STAT5A

We next used siRNA to knock down Rac1 or MgcRacGAP expression in Ba/F3 cells where STAT5 activation is required for cell growth. The siRNA treatment for Rac1 or MgcRacGAP resulted in severe growth retardation of Ba/F3 cells and caused apoptosis in some cells. The total cell number was only one tenth or one fifth 48 h after siRNA treatment for Rac1 or MgcRacGAP, respectively (unpublished data). The siRNA treatment for MgcRacGAP led to the formation of multinucleated cells, as reported previously (Mishima et al., 2002), but no more than 20% of the cells, indicating the failure of cytokinesis by MgcRacGAP depletion is not the major cause of the growth inhibition.

We then did semiquantitative RT-PCR analysis to test whether transcriptional activation of STAT5 is affected by the knock down of Rac1 or MgcRacGAP and found that expression of bcl-xL, one of the STAT5 target genes, was severely impaired by the siRNA treatment (Fig. 4 A). We also confirmed that siRNA treatments specifically decreased the expression levels of Rac1 or MgcRacGAP protein but not those of RhoA and HDAC, similar to the results shown in Fig. 4 B (not depicted).

We also investigated whether knock down of Rac1 or MgcRacGAP affects the subcellular distribution of STAT5A and p-STAT5A in Ba/F3 cells before and after IL-3 stimulation. The siRNA-treated Ba/F3 cells were starved for 6 h after the isolation of live cells using Ficoll and stimulated with IL-3 (15 min), and the cell lysates were fractionated. The siRNA treatments specifically decreased expression levels of Rac1 or MgcRacGAP protein (Fig. 4 B, c and d) but not those of RhoA and HDAC (Fig. 4 B, e and f). The IL-3–induced nuclear accumulation of STAT5A and p-STAT5A was almost completely blocked in Ba/F3 cells treated with either Rac1 or MgcRacGAP siRNA when compared with those treated with the control siRNA (Fig. 4 B, a and b). The same treatment moderately decreased the amounts of p-STAT5A and total STAT5A in the cytoplasmic fraction (Fig. 4 B, a and b), suggesting that Rac1 and MgcRacGAP enhance the IL-3–induced phosphorylation of STAT5A and somehow stabilize STAT5A in the cytoplasm.

Direct interaction between STATs and MgcRacGAP/Rac1 regulates the activation of STATs through facilitating their tyrosine phosphorylation and nuclear translocation

We previously found that STAT3 bound MgcRacGAP through its DBD (Tonozuka et al., 2004). To examine whether MgcRacGAP regulated transcriptional activity of STAT3 and -5A through direct interaction, we attempted to produce mutant STATs lacking

Published December 18, 2006

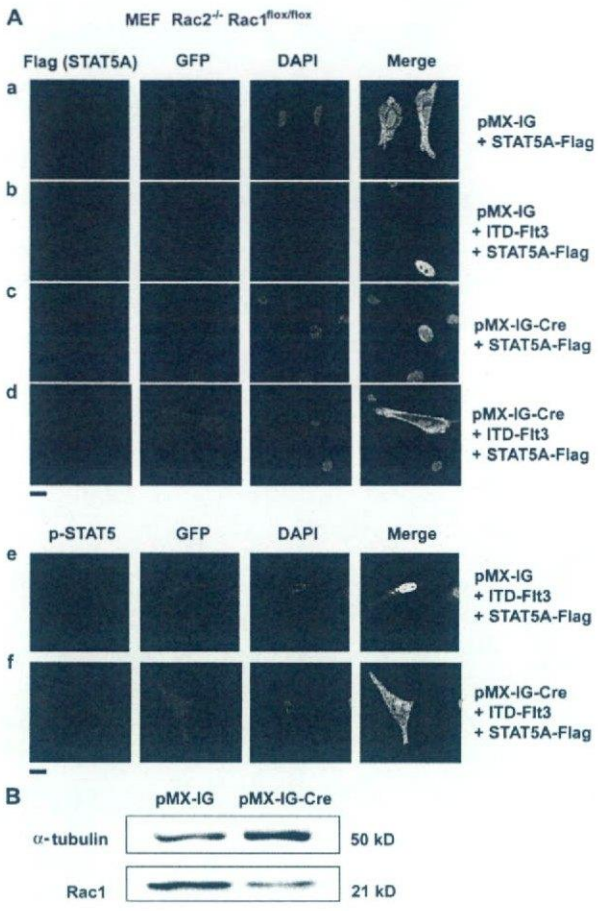

Figure 3. **The nuclear translocation of p-STAT5 was not observed in the Rac1-knockout mouse embryonic fibroblasts.** (A) The nuclear translocation of ITD-Flt3–induced p-STAT5 was impaired in the Rac2 $^{-/-}$ Rac1$^{flox/flox}$ fibroblasts. The Rac2 $^{-/-}$ Rac1$^{flox/flox}$ fibroblasts were transduced with a control pMX-IG (a and b) or pMX-IG-Cre (c and d) retrovirus vector. After 3 d, cells were transiently cotransfected with pME/STAT5A-Flag and MOCK (a and c) or pMKIT/ITD-Flt3 (b and d). After 36 h, the cells were fixed and immunostained with the anti-Flag antibody (a–d, left) or anti–p-STAT5 antibody (e and f, left). Bars, 10 μm. (B) Expression of Rac1 was depleted in the Rac2 $^{-/-}$ Rac1$^{flox/flox}$ fibroblasts by Cre recombinase. Expression of α-tubulin and Rac1 was examined in the Rac2 $^{-/-}$ Rac1$^{flox/flox}$ fibroblasts retovirally transduced with a control pMX-IG or pMX-IG-Cre.

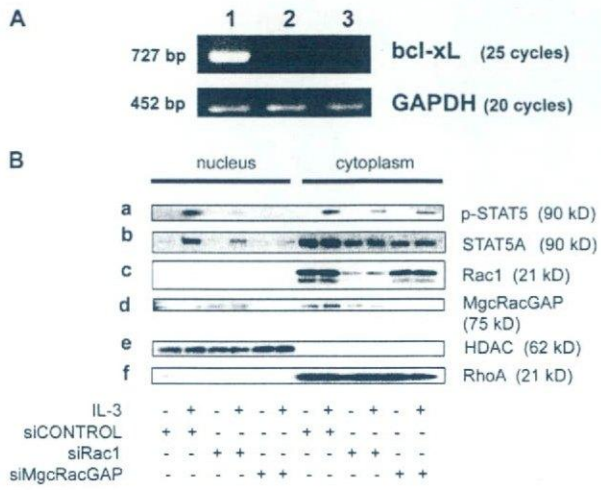

Figure 4. **Rac1 and MgcRacGAP were required for IL-3–induced nuclear accumulation and transcriptional activation of p-STAT5A.** (A) IL-3–induced transcriptional activation of STAT5A was suppressed by knock down of Rac1 or MgcRacGAP. Expression of bcl-xL or GAPDH mRNA was examined in Ba/F3 cells treated with the control siRNA (lane 1), Rac1 siRNA (lane 2), or MgcRacGAP siRNA (lane 3). 24 h after the siRNA treatment, the live cells were collected using Ficoll and subjected to semiquantitative RT-PCR. (B) IL-3–induced nuclear accumulation of p-STAT5A was impaired by knock down of Rac1 or MgcRacGAP. The intracellular distribution of p-STAT5A or total STAT5A in the IL-3–stimulated or unstimulated Ba/F3 cells pretreated with the control, Rac1, or MgcRacGAP siRNA (a and b). Note that Rac1 or MgcRacGAP expression was specifically suppressed by siRNA (c and d). Cytosol and nuclear extracts were prepared as described previously (Nakamura et al., 2002) and validated by Western blot using an anti-HDAC antibody or anti-RhoA antibody (e and f).

the MgcRacGAP binding site. To this end, we narrowed down the binding site in DBD-STAT3 to a 25-amino-acid stretch, using MBP-fused DBD-STAT3 truncations (DB1-DB6; Fig. S3 A, available at http://www.jcb.org/cgi/content/full/jcb.200604073/DC1). We found that only DB2 (aa 338–362) of DBD-STAT3 interacted with MgcRacGAP (Fig. S3 B). Conversely, the mutant of DBD-STAT3 lacking DB2 (DBD-STAT3-dDB2) did not bind MgcRacGAP (Fig. S3 C). These results clearly demonstrated that the DB2 region (25 amino acid) of STAT3 bound MgcRacGAP. This region is well conserved among STAT family proteins and harbors a β-sheet structure, which is thought to mediate protein–protein interaction. Purified MgcRacGAP was pulled down by the MBP-DB2 of STAT3, and the corresponding region of STAT5 (aa 341–365) fused with MBP but not by MBP alone, demonstrating that MgcRacGAP directly bound DB2 of STAT3 and -5 (Fig. S3 D and Fig. 5 A). Both of the STAT3 and -5A mutants lacking DB2 (STAT3- and STAT5A-dDB2) did not bind MgcRacGAP and the extent of tyrosine phosphorylation of these mutants was less prominent after IL-6 or ITD-Flt3 stimulation (Fig. 5 B and not depicted). In addition, STAT3- and STAT5A-dDB2 lacked their transcriptional activities (Fig. S3 E and Fig. 5 C). These results indicated that the interaction of MgcRacGAP/Rac1 with STAT3 and -5A facilitates cytokine receptor–induced tyrosine phosphorylation of both STAT3 and -5A. Considerable decrease in the tyrosine phosphorylation of STAT5A was also observed when Rac1 or MgcRacGAP was knocked down (Fig. 4 B, a). Intriguingly, MgcRacGAP also interacted with JAK2 (Fig. 5 D), suggesting that MgcRacGAP/Rac1 also mediated the tyrosine phosphorylation of STATs through the interaction with JAK2. Importantly, STAT3- and STAT5A-dDB2 that do not bind MgcRacGAP did not enter the nucleus even after tyrosine phosphorylation by IL-6 or ITD-Flt3 (Fig. 5 E and not depicted), suggesting that MgcRacGAP/Rac1 is required not only for nuclear translocation of p-STATs but also for efficient tyrosine phosphorylation of STATs.

MgcRacGAP and GTP-bound Rac1 were required for the nuclear translocation of p-STAT5A in cytosol-free digitonin-permeabilized cells

We established a nuclear transport assay using semi-intact permeabilized cells (Adam et al., 1990), which enables us to

Published December 18, 2006

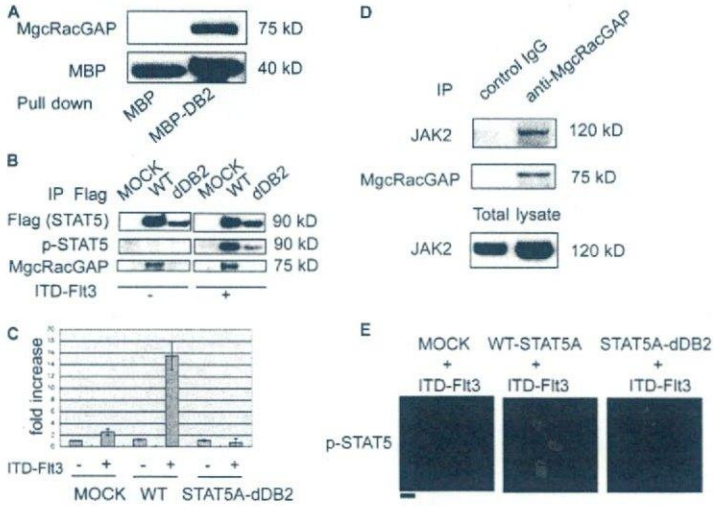

Figure 5. **The mutant of STAT5A, which lacks MgcRacGAP binding site, was not efficiently tyrosine phosphorylated by ITD-Flt3 stimulation and did not enter the nucleus even after tyrosine phosphorylation.** (A) The DB2 region of STAT5 directly interacted with MgcRacGAP in vitro. Full-length MgcRacGAP was expressed in Sf-9 cells using the baculovirus vector and was purified from infected Sf-9 cells. The recombinant MgcRacGAP was pulled down by MBP-DB2 or MBP-bound beads and subjected to Western blot analysis with the anti-MgcRacGAP (top) or anti-MBP antibody for the loading control (bottom). (B) The deletion mutant of DB2 did not bind MgcRacGAP, and the STAT5 phosphorylation was considerably impaired by the deletion of DB2. Expression and tyrosine phosphorylation of Flag-tagged STAT5A-dDB2 (top and middle, respectively) were examined in the MOCK or ITD-Flt3–transfected 293T cells. The interactions of MgcRacGAP with the WT-STAT5A or STAT5A-dDB2 were also examined in the MOCK or ITD-Flt3–transfected 293T cells (bottom). Images of the immunoblots using the MOCK or ITD-Flt3–transfected cells are derived from the same exposure of one gel that was cut to remove intervening lanes. (C) The transcriptional activity of STAT5-dDB2 was impaired. Luciferase activities were examined in the lysates of ITD-Flt3–stimulated 293T cells cotransfected with the STAT5-reporter plasmid together with internal control reporter plasmids and the MOCK vector (pME), the expression vector for the Flag-tagged WT-STAT5, or STAT5-dDB2 mutant. The results shown are the mean ± SD of three independent experiments. (D) MgcRacGAP was coprecipitated with JAK2. The cell lysates of 293T cells transfected with the expression vector (pRK5) for JAK2 were subjected to immunoprecipitation with the anti-MgcRacGAP or control antibody, followed by the immunoblotting with the anti-JAK2 (top) or anti-MgcRacGAP antibody (middle). Levels of transfected JAK2 were assayed by blotting with the anti-JAK2 antibody (bottom). (E) STAT5A-dDB2 did not enter the nucleus even after the phosphorylation. The 293T cells were cotransfected with pMKIT/ITD-Flt3 together with the MOCK (left), the expression vector for the Flag-tagged WT-STAT5A (middle), or STAT5A-dDB2 (right). After 24 h, the cells were fixed and immunostained with the anti–p-STAT5 antibody. Bar, 10 μm.

biochemically analyze the roles of Rac1 and MgcRacGAP in the nuclear import of p-STAT5A. We confirmed the purities of STAT5A, MgcRacGAP, V12Rac1, N17Rac1, importin α1, importin α5, importin β1, Ran, and NTF2 produced by Sf-9 cells, and the tyrosine phosphorylation of STAT5A induced by coexpression with the kinase domain of JAK2 in Sf-9 cells (Fig. 6, A and B). It was confirmed that the purified p-STAT5A bound DNA in electrophoretic mobility shift analysis (EMSA) in a similar fashion with GM-CSF–activated STAT5 in TF-1 cells (Fig. S4 A, available at http://www.jcb.org/cgi/content/full/jcb.200604073/DC1), indicating that the recombinant in vivo phosphorylated STAT5A formed a proper dimer. Permeabilized HeLa cells were incubated with the indicated combinations of purified proteins in transport buffer (TB) plus an energy regenerating system. After the import reaction in the cells incubated with purified unphosphorylated STAT5A, a considerable amount of unphosphorylated STAT5A was detected at the cytoplasm in most cells (Fig. 6 C, a). The addition of purified MgcRacGAP, V12Rac1, importin α1, and importin β1 did not affect localization of unphosphorylated STAT5A (Fig. 6 C, b–d and f). Although rabbit reticulocyte lysate reduced cytoplasmic localization of unphosphorylated STAT5A (Fig. 6 C, e), it induced both the nuclear and plasma membrane localization of p-STAT5A (Fig. 6 C, k). These results suggested that rabbit reticulocyte lysate contained cofactors that are required for the nuclear translocation of p-STAT5A in this transport assay. Interestingly, p-STAT5A accumulated at the nuclear membrane, with some migrating into the nucleus in the presence of purified MgcRacGAP and V12Rac1, but the nuclear translocation of p-STAT5A was inhibited in the presence of purified MgcRacGAP and N17Rac1 (Fig. 6 C, h and i). These results indicate that the GTP-bound form of Rac1 and MgcRacGAP facilitate the nuclear translocation of p-STAT5A. Given that purified importin β1 also accumulated mostly in the nuclear envelope and only partially migrated to the nucleus in our assay system (unpublished data) as reported previously (Kutay et al., 1997), the accumulation of p-STAT5 and importin β1 in the nucleus might have been caused by residual amounts of nuclear transporters left in the assay system. Thus, it is likely that the GTP-bound form of Rac1 and MgcRacGAP play critical roles in targeting p-STAT5A to the nuclear envelope and that cofactors are required for the efficient nuclear import of p-STAT5A from the nuclear envelope. In fact, nuclear translocation of p-STAT5A was enhanced by further addition of the purified nuclear transporters, including importin α1, importin β1, Ran, and NTF2 to the assay (Fig. 6 C, j). This nuclear translocation of p-STAT5A was not observed in the absence of MgcRacGAP even in the presence of cofactors (Fig. 6 C, l).

To confirm whether the unphosphorylated recombinant STAT5A conserved a native folded state, we did nuclear transport assay using the in vitro phosphorylated STAT5A. The recombinant full-length JAK2 efficiently phosphorylated the recombinant STAT5A in the kinase reaction buffer (Fig. S4 B). This in vitro phosphorylated STAT5A behaved in the nuclear transport assay like the in vivo phosphorylated STAT5A (Fig. S5, a–i, available at http://www.jcb.org/cgi/content/full/jcb.200604073/DC1). The nuclear transport of p-STAT5A requires both MgcRacGAP and V12Rac1. The nuclear import of the in vitro phosphorylated recombinant STAT5A was also achieved by the presence of the cytosol fraction of HeLa cells (HeLa-CS), which had been prepared as described previously (Adam et al., 1990). In addition, immunodepletion of MgcRacGAP or Rac1 considerably inhibited the nuclear import of the in vitro phosphorylated recombinant STAT5A (Fig. S5, j–m). This inhibition

Published December 18, 2006

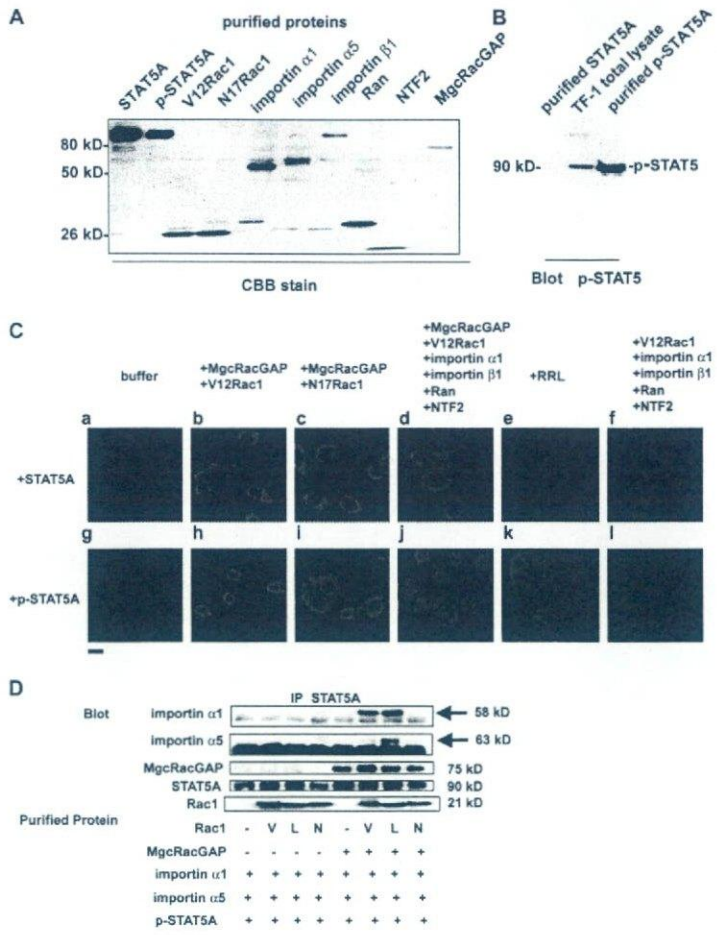

Figure 6. **Purified p-STAT5A accumulated to the nuclear envelope in the presence of V12Rac1 and MgcRacGAP in the nuclear transport assay.** (A) Coomassie blue (CBB) staining of purified STAT5A, p-STAT5A, V12Rac1, N17Rac1, importin α1, importin α5, importin β1, Ran, NTF2, or MgcRacGAP. (B) Western blot analysis of the STAT5A-Flag protein purified from Sf-9 cells with or without coexpression with the kinase domain of JAK using the anti–p-STAT5 antibody. Total cell lysate of GM-CSF–stimulated TF-1 was used as a control. (C) The nuclear transport assay. HeLa cells were permeabilized with 40 μg/ml digitonin. Incubation with 50 μl import mix was done at 37°C for 30 min. Import mix contained TB, an energy regenerating system, and a single or combinations of the following purified proteins as indicated: 1 μM STAT5A, p-STAT5A, V12Rac1, N17Rac1, MgcRacGAP, importin α1, importin β1, Ran, or NTF2. After the import reaction, the cells were fixed. STAT5A protein was detected using the anti-STAT5A antibody. Cells were examined using a Fluoview FV300 confocal microscope. A representative result of three independent experiments is shown. Bar, 10 μm. (D) The direct bindings of both GTP-bound Rac1 and MgcRacGAP facilitated the interaction of p-STAT5A with importin αs. Purified p-STAT5A was incubated with importin αs in the absence or presence of the indicated combinations of V12Rac1, L61Rac1, N17Rac1, or MgcRacGAP in TB containing 5% BSA to block nonspecific bindings. 1 μg of each purified protein was used for each sample. After the incubation for 30 min at RT, STAT5A was immunoprecipitated with anti-STAT5A antibody and washed three times with TB. The immunoprecipitates were subjected to Western blot analysis with the anti–importin α1, anti–importin α5, anti-Rac1, anti-MgcRacGAP, or anti-STAT5A antibody.

was restored by add-back of the purified recombinant MgcRacGAP or Rac1 (Fig. S5, n and o).

To determine whether the Rac1 activation or the presence of MgcRacGAP is required for the interaction of p-STAT5A with importin αs, an in vitro binding assay was done using purified proteins. Intriguingly, p-STAT5A formed complexes with importin α1 and α5 only in the presence of both MgcRacGAP and V12Rac1 or another constitutively active mutant L61Rac1, but not N17Rac1 (Fig. 6 D). These results demonstrated that GTP-bound Rac1 and MgcRacGAP functions as p-STAT5A nuclear chaperone, facilitating p-STAT5A to form protein complexes with importin αs.

Discussion

In the present work, we demonstrate that Rac1 and MgcRacGAP are essential for the nuclear translocation of STAT5A, based on the following observations. First, Rac1 and MgcRacGAP directly bound STAT5A, and the interaction between MgcRacGAP and STAT5A was enhanced by IL-3 stimulation. Second, STAT5A and MgcRacGAP simultaneously entered the nucleus upon IL-3 and ITD-Flt3 stimulation. Third, knock down of Rac1 or MgcRacGAP profoundly inhibited both the IL-3–induced transcriptional activation of STAT5A and the nuclear accumulation of p-STAT5A in IL-3–dependent Ba/F3 cells. Fourth, depletion of Rac1 in fibroblasts, as well as expression of N17Rac1 in 293T cells, prevented p-STAT5A from entering the nucleus. Fifth, p-STAT5A lacking the MgcRacGAP binding site (p-STAT5A–dDB2) did not accumulate in the nucleus. Last, in a nuclear transport assay, purified V12Rac1 and MgcRacGAP induced accumulation of purified p-STAT5A on the nuclear envelope, with some p-STAT5A migrating into the nucleus, and the further addition of nuclear transporters, including importin α1, importin β1, Ran, and NTF2, achieved the efficient nuclear translocation of p-STAT5A. Moreover, either the absence of MgcRacGAP or the presence of N17Rac1 inhibited this nuclear translocation of p-STAT5A.

Simon et al. (2000) suggested that an active form but not an inactive form of Rac1 bound STAT3 and played important roles in EGF-induced STAT3 activation. These authors did not, however, specifically examine the nuclear transport of STAT3. Interestingly, EGF receptor–mediated endocytosis is required for cytoplasmic transport of STAT3 (Bild et al., 2002), and MgcRacGAP is recruited to the EGF receptor complex after EGF stimulation (Blagoev et al., 2003). We also found that STAT3 bound Rac1 and Rac2, which was enhanced by IL-6 stimulation.

Published December 18, 2006

In addition, STAT3 bound MgcRacGAP, which was required for the transcriptional activation of STAT3, and some population of MgcRacGAP entered the nucleus together with STAT3 (Tonozuka et al., 2004). Although these results suggested a role of Rac1/MgcRacGAP in STAT3 activation, the underlying molecular mechanisms remained elusive. We studied the functional interactions using a nuclear transport assay and found that the nuclear translocation of p-STAT3 as well as p-STAT5A was induced in the presence of a combination of purified proteins, including V12Rac1, MgcRacGAP, importin α1, importin β1, Ran, and NTF2 (Fig. 6, Fig. S5, and not depicted). These results demonstrate a novel Rac1 function in the nuclear transport of p-STAT3 as well as p-STAT5A.

Although we showed the results for STAT5A, we obtained identical results in experiments so far performed for closely related STAT5B (unpublished data). In addition, the phenotypes of STAT3- and STAT5A-dDB2 were nearly identical (Fig. 5 and Fig. S3), and the region of STAT3 that binds to MgcRacGAP (STAT3-DBD-DB2) is well conserved among STAT family proteins, suggesting a general role for MgcRacGAP and Rac1 in the nuclear transport of p-STAT proteins.

Involvement of Rac1 in the nuclear transport of STATs

The Rho family small GTPases play key roles in a variety of cellular functions, including regulation of cell cycle, transcription, and transformation (Bishop and Hall, 2000). Among them, the Rac subfamily consists of three known members: Rac1, Rac2, and Rac3. Although Rac1 and Rac3 are ubiquitously expressed, Rac2 expression is specific in hematopietic cells. Rac1 and Rac2 were implicated in both distinct and overlapping functions, including cell migration, membrane ruffling, production of superoxide, and phagocytosis (Ridley, 1995; Roberts et al., 1999; Bishop and Hall, 2000; Williams et al., 2000; Gu et al., 2003; Cancelas et al., 2005). Interestingly, the C-terminal region of Rac1 but not Rac2 or Rac3 contained a functional NLS, suggesting a role for Rac1 in the nucleus. Consistent with this, Rac1 was reported to play a role in the nuclear import of SmgGDS and p120 catenin (Lanning et al., 2003), members of the importin α–like armadillo family of proteins (Peifer et al., 1994; Chook and Blobel, 2001). In the present paper, using Rac1-deficient mouse embryonic fibroblasts, we demonstrate that Rac1 was critically required for the nuclear transport of p-STAT5A (Fig. 3).

Requirement of cofactors involved in importin α/β pathway for nuclear import of STAT5

It was reported that unphosphorylated STATs shuttled between the cytoplasm and nucleus (Zeng et al., 2002; Marg et al., 2004). Activated STAT1 was reported to bind importin α5, leading to its nuclear translocation (Sekimoto et al., 1997; McBride et al., 2002). How activated STAT3 is imported to the nucleus has remained controversial. Ushijima et al. (2005) showed that activated STAT3 binds importin α1, α3, and α5, and Ma and Cao (2006) demonstrated that activated STAT3 binds importin α5 and α7 but not α1, α3, or α4, whereas Liu et al. (2005) reported that STAT3 nuclear import is independent of tyrosine phosphorylation and mediated by importin α3. On the other hand, how activated STAT5A is imported to the nucleus remained largely elusive. It was reported that the ERBB4/HER4 receptor tyrosine kinase, which harbors the NLS sequence, functions as a STAT5A nuclear chaperone, implicating the NLS of STAT5A-associated molecules in the nuclear translocation of STAT5A (Williams et al., 2004). However, unlike ERBB4/HER4, ITD-Flt3 does not harbor an NLS and did not enter the nucleus (unpublished data). In the nuclear transport assay, most p-STAT5A accumulated to the nuclear envelope in the presence of V12Rac1 and MgcRacGAP, and further addition of the purified nuclear transporters, including importin α1, importin β1, Ran, and NTF2, facilitated the nuclear translocation of p-STAT5A (Fig. 6 C, j). Together, it is likely that the complex of p-STAT5, GTP-bound Rac1, and MgcRacGAP translocates to the nuclear envelope, where it recruits other factors such as importin α/β to pass through the nuclear pore complex into the nucleus. Indeed, direct interaction of both GTP-bound Rac1 and MgcRacGAP facilitated the interaction of p-STAT5A with importin αs (Fig. 6 D). In agreement with this, Rac1 harbors an NLS (Lanning et al., 2003) and MgcRacGAP harbors a bipartite NLS and binds importin αs (unpublished data). Interestingly, a mutant of MgcRacGAP lacking NLS strongly blocked the nuclear translocation of p-STATs in the nuclear transport assay even with V12Rac1, importin α1, importin β1, Ran, and NTF2 (unpublished data), suggesting a role of MgcRacGAP as an NLS-containing nuclear chaperone of p-STATs. Establishment of the nuclear transport assay for p-STATs has enabled us to clearly demonstrate the requirement of Rac1 and MgcRacGAP for the nuclear translocation of p-STATs.

The activities of small GTPases are regulated by two classes of proteins, GAPs and GEFs (guanine nucleotide exchange factors). In this paper, we did not address GEFs, but some, such as smgGDS or ECT-2, may also participate in the nuclear transport of STAT proteins. Based on the results that p-STAT5A binds importin αs only in the presence of MgcRacGAP and active forms of Rac1 but not inactive form of Rac1, we speculate that Rac1 inactivation by MgcRacGAP release p-STATs from the importin complex in the nucleus. To prove this hypothesis and clarify its molecular mechanisms, further work will be required.

Coordinate control of cell division and transcription

Another interesting question raised by our work concerns the coordinate control of cell division and transcription. We originally identified MgcRacGAP as a GAP protein that regulates IL-6–induced macrophage differentiation of leukemic M1 cells (Kawashima et al., 2000). Later, we and others found that MgcRacGAP or Cyk-4, an orthologue in *Caenorhabditis elegans*, played essential roles in cytokinesis (Jantsch-Plunger et al., 2000; Hirose et al., 2001; Van de Putte et al., 2001; Mishima et al., 2002). We further demonstrated that MgcRacGAP was phosphorylated at Serine 387 by Aurora-B at the midbody, functionally converted from Rac/Cdc42-GAP to Rho-GAP, and played essential roles to complete cell division in cytokinesis (Minoshima et al., 2003). In interphase, MgcRacGAP formed a

Published December 18, 2006

complex with Rac1 and STAT3 and was required for the full transcriptional activation of STAT3, thereby enhancing the differentiation of IL-6–stimulated M1 cells (Tonozuka et al., 2004). On the other hand, when STAT5 was activated by IL-3 or ITD-Flt3 in conjunction with Rac1 and MgcRacGAP, the cells proliferate. Thus, MgcRacGAP functions as a Rac-GAP to activate transcription of STAT in the nucleus of interphase cells, probably leading to cell proliferation or differentiation. At cytokinesis, it functions as a Rho-GAP to complete cytokinesis, indicating that the distinct roles of the Rho family small GTPases depend on the cell cycle.

Does Rac1 play a general role in nuclear transport of transcription-related proteins?

The experiments using N17Rac1 showed that Rac1 contributes to maximal activation of STAT1 and -3 in response to IFN-γ (Park et al., 2004). The molecular mechanisms of this phenomenon can be explained by our current results. Esufali and Bapat (2004) suggested that Rac1 plays some role in redistribution of β-catenin and that a mutant Rac1 lacking its NLS hampers nuclear localization of β-catenin, leading to attenuation of the β-catenin–dependent transcriptional activity of T cell factor/lymphoid enhancing factor. The authors stated that it was not yet clear whether the Rac1/β-catenin association facilitated nuclear import or retention of β-catenin or, alternatively, Rac1 augments the function of β-catenin as a coactivator. Given the results of the present study, however, it is likely that Rac1 also plays a critical role in the nuclear transport of β-catenin, suggesting a general role of Rac1 GTPase for the nuclear transport of transcription factors. It is tempting to speculate that Rac1 is a molecular link between changes in cytoskeletal organization and alterations in transcription.

Materials and methods

Culture, cytokines, and antibodies

Ba/F3 cells were maintained in RPMI1640 medium (Invitrogen) containing 10% FCS and 1 ng/ml mIL-3 (R&D Systems). An ecotropic retrovirus packaging cell line PLAT-E was maintained as described previously (Hirose et al., 2001). An anti-STAT5A antibody and anti-STAT5B antibody were obtained from R&D Systems. Affinity-purified anti-MgcRacGAP antibody was produced as described previously (Hirose et al., 2001). An anti-Rac1 mAb and anti–importin α1 mAb were purchased from BD Biosciences. The rabbit polyclonal anti-Rac1, anti-RhoA, anti-JAK2, and goat polyclonal anti-HDAC or anti–importin α5 antibodies were obtained from Santa Cruz Biotechnology, Inc.

Immunoprecipitation and Western blotting

Immunoprecipitation, gel electrophoresis, and immunoblotting were done as described previously (Kawashima et al., 2001), with minor modifications. Cell lysates (2×10^7 cells/ml) were incubated at 4°C for 2 h with the indicated antibodies and protein A–Sepharose. The immunoprecipitates were subjected to Western blot analysis with an anti–p-STAT5 mAb (Upstate Biotechnology), anti-MgcRacGAP, or anti-STAT5A antibody. The loading amounts were verified with the anti-STAT5A or anti-MgcRacGAP antibody after stripping the filters. The filter-bound antibody was detected using the ECL system (GE Healthcare). Cytosol and nuclear fractions were prepared as described previously (Nakamura et al., 2002).

MBP pull-down assays

MBP fusion proteins (0.5 μg) bound to amylose resin beads were incubated with cell lysates (10 μg) from IL-3–stimulated Ba/F3 cells as described previously (Tonozuka et al., 2004).

Transfection and immunostaining

The 293T cells were transfected with 1.0 μg pME/STAT5A-Flag together with 0.5 μg pMKIT (MOCK) or pMKIT/ITD-Flt3, and in some experiments cells were transfected with 0.5 μg pME/STAT5A-HA and 0.5 μg pMKIT (MOCK) or pMKIT/ITD-Flt3 together with 1.0 μg pCMV5/N17Rac1-Flag, using Lipofectamine Plus reagents (Life Technologies). After 24 h, cells were plated on glass coverslips, and the next day the cells were immunostained as described previously (Hirose et al., 2001).

Microscopy

Fluorescence images were analyzed on a confocal microscope (Fluoview FV300 Scanning Laser Biological Microscope IX 70 system; Olympus) equipped with two lasers (Ar 488 and HeNe 543) using a 60× oil objective (PlanApo; Olympus). Fluoview version 4.3 software (Olympus) was used for image acquisition from confocal microscopy. Photoshop 7.0 or Photoshop Elements 2.0 software (Adobe) was used for processing of images.

RNA interference and semiquantitative RT-PCR

For the silencing of Rac1 or MgcRacGAP, SMARTpool Rac1 or MgcRacGAP siRNA (L-041170 or L040081; Dharmacon) was used. A control siRNA was used as a nonsilencing control (Tonozuka et al., 2004). 5 μl of 40 μM double-stranded siRNA were introduced in to 2×10^6 cells of Ba/3F cells with Nucleofector II (Amaxa) set at program T-16 using a Cell Line Nucleofector kit V (Amaxa) according to the manufacturer's instruction. A control vector carrying GFP was introduced to >80% of Ba/3F cells under this condition. 24 h after transfection, live cells were isolated using Ficoll-Paque PLUS (GE Healthcare), and gene expression was examined by semiquantitative RT-PCR analysis as described previously (Nosaka et al., 1999). The primers used are as follows: 5′bcl-x, 5′-GAAAGAATTCACCATGTCTCAGAGCAACCGG-3′; 3′bcl-x, 5′-GAAAGCGGCCGCTCACTTCCGACTGAAGAGTG-3′; 5′GAPDH, 5′-ACCACAGTCCATGCCATCAC-3′; 3′GAPDH, 5′-TCCACCACCCTGTTGCTGTA-3′.

Production of retroviruses

High-titer retroviruses harboring Cre recombinase were produced in a transient retrovirus packaging cell line PLAT-E (Morita et al., 2000) and were used to deplete Rac1 in Rac2$^{-/-}$ Rac1$^{flox/flox}$ fibroblasts (Fig. 3 B).

Generation, expression, and purification of recombinant proteins in Sf-9 cells

To construct baculovirus vectors, the cDNAs encoding STAT5A, MgcRacGAP, V12Rac1, L61Rac1, N17Rac1, importin αs, importin β1, Ran, and NTF2 with the C-terminal Flag epitope tag, and a kinase domain of JAK2 (JH1; Saharinen et al., 2000) were subcloned into pBacPAK (BD Biosciences). The resulting constructs were used to obtain recombinant baculoviruses by cotransfection with Bsu36 I–digested BacPAK viral DNA (BD Biosciences) into Sf-9 cells according to the manufacturer's protocol. For protein expression, Sf-9 cells were infected with high-titer viral stocks for 96 h and lysed. The lysate was clarified by centrifugation, and the supernatant was immunoprecipitated with the anti-Flag M2-agarose affinity gel (Sigma-Aldrich) for 2 h at 4 °C. The recombinant Flag-tagged proteins were eluted with 3× Flag peptide (Sigma-Aldrich).

EMSA using purified p-STAT5A

To determine whether purified p-STAT5A formed a proper dimer, EMSA was performed using consensus sequence of STAT5A as a probe, as described previously (Kawashima et al., 2001).

In vitro kinase reaction

An in vitro kinase reaction of purified STAT5A was performed as described previously with minor modifications (Quelle et al., 1995). In vitro phosphorylated STAT5A was immunoprecipitated with the anti-Flag M2-agarose affinity gel and reeluted with a 3× Flag peptide. The purified in vitro phosphorylated STAT5A was dialyzed against TB, and the final concentrations of STAT5A protein were determined for use in SDS-PAGE and in the nuclear transport assay.

Preparation of fluorescent conjugates

FITC-labeled BSA (Sigma-Aldrich) conjugated with a synthetic peptide containing the SV40 large T antigen (CGGGPKKKRKVED; NLS-conjugated FITC-BSA) was prepared as described previously (Adam et al., 1990), as a control protein harboring an NLS. We confirmed that NLS-conjugated FITC-BSA was imported to the nucleus in our experimental conditions as reported previously (Kutay et al., 1997), which was not inhibited by immunodepletion of MgcRacGAP or Rac1 (Fig. S5, p–t).

Import assays with permeabilized cells

HeLa cells were grown on poly-L-lysine–coated coverslips and permeabilized with 40 μg/ml digitonin (Roche) in TB (20 mM Hepes, pH 7.3, 110 mM KOAC, 2 mM $Mg(OAC)_2$, 1 mM EGTA, 2 mM DTT, 0.4 mM PMSF, 3 μg/ml aprotinin, 2 μg/ml pepstatin A, 1 μg/ml leupeptin, and 20 mg/ml BSA) for 10 min at RT. Subsequently, the cells were washed twice in TB. Incubation with 50 μl import mix was performed at 37°C for 30 min. The import mix contained TB, an energy regenerating system (0.5 mM ATP, 0.5 mM GTP, 10 mM creatine phosphate, and 30 U/ml creatine phosphokinase), and 1 μM of purified unphosphorylated or phosphorylated STAT5A alone, or STAT5A plus the 1 μM of other purified cofactor proteins as indicated in Fig. 6 C. After the import reaction, the cells were washed with ice-cold TB and immunostained with the anti-STAT5A antibody and anti–p-STAT5 mAb as described previously (Hirose et al., 2001). Fixed cells were examined using a Fluoview FV300 confocal microscope (Olympus).

Online supplemental material

Fig. S1 depicts the binding domains of MgcRacGAP with STAT5A and that of STAT5A with MgcRacGAP. Fig. S2 shows that N17Rac1 expression inhibits the nuclear translocation of p-STAT5A. Fig. S3 shows that the DB2 region is required for the interaction of STAT3 with MgcRacGAP and the transcriptional activation of STAT3. Fig. S4 shows that purified p-STAT5A forms a dimer and binds DNA containing the STAT5 consensus sequence and that the purified STAT5A can be phosphorylated in vitro. Fig. S5 shows that the in vitro phosphorylated recombinant STAT5A can be imported to the nucleus in the nuclear transport assay and that immunodepletion of Rac1 or MgcRacGAP specifically inhibits the nuclear import of p-STAT5A using HeLa cytosol extract. Online supplemental material is available at http://www.jcb.org/cgi/content/full/jcb.200604073/DC1.

We thank Dr. Y. Kaziro for critical reading of the manuscript, Dr. T. Satoh for valuable discussions, and M. Ohara and Dovie Wylie for language assistance. We also thank R&D Systems for providing us with cytokines.

This work was supported by grants from the Ministry of Education, Science, Sports and Culture of Japan (16209 032) and a grant in aid from the Sumitomo Foundation. The Division of Hematopoietic Factors is supported by the Chugai Pharmaceutical Co., Ltd. David A. Williams was supported by grants from the National Institutes of Health (R01 DK62757).

Submitted: 13 April 2006
Accepted: 20 November 2006

References

Adam, S.A., R.S. Marr, and L. Gerace. 1990. Nuclear protein import in permeabilized mammalian cells requires soluble cytoplasmic factors. *J. Cell Biol.* 111:807–816.

Bild, A.H., J. Turkson, and R. Jove. 2002. Cytoplasmic transport of Stat3 by receptor-mediated endocytosis. *EMBO J.* 21:3255–3263.

Bishop, A.L., and A. Hall. 2000. Rho GTPases and their effector proteins. *Biochem. J.* 348:241–255.

Blagoev, B., I. Kratchmarova, S.E. Ong, M. Nielsen, L.J. Foster, and M. Mann. 2003. A proteomics strategy to elucidate functional protein-protein interactions applied to EGF signaling. *Nat. Biotechnol.* 21:315–318.

Bromberg, J.F., M.H. Wrzeszczynska, G. Devgan, Y. Zhao, R.G. Pestell, C. Albanese, and J.E. Darnell Jr. 1999. The JAK-STAT pathway: summary of initial studies and recent advances. Stat3 as an oncogene. *Cell.* 98:295–303.

Cancelas, J.A., A.W. Lee, R. Prabhakar, K.F. Stringer, Y. Zheng, and D.A. Williams. 2005. Rac GTPases differentially integrate signals regulating hematopoietic stem cell localization. *Nat. Med.* 11:886–891.

Chook, Y.M., and G. Blobel. 2001. Karyopherins and nuclear import. *Curr. Opin. Struct. Biol.* 11:703–715.

Darnell, J.E., Jr. 1996. The JAK-STAT pathway: summary of initial studies and recent advances. *Recent Prog. Horm. Res.* 51:391–403.

Darnell, J.E., Jr. 2002. Transcription factors as targets for cancer therapy. *Nat. Rev. Cancer.* 2:740–749.

Debreceni, B., Y. Gao, F. Guo, K. Zhu, B. Jia, and Y. Zheng. 2004. Mechanisms of guanine nucleotide exchange and Rac-mediated signaling revealed by a dominant negative trio mutant. *J. Biol. Chem.* 279:3777–3786.

Esufali, S., and B. Bapat. 2004. Cross-talk between Rac1 and dysregulated Wnt signaling pathway leads to cellular redistribution of β-catenin and TCF/LEF-mediated transcriptional activation. *Oncogene.* 23:8260–8271.

Gu, Y., M.D. Filippi, J.A. Cancelas, J.E. Siefring, E.P. Williams, A.C. Jasti, C.E. Harris, A.W. Lee, R. Prabhakar, S.J. Atkinson, et al. 2003. Hematopoietic cell regulation by Rac1 and Rac2 guanosine triphosphatases. *Science.* 302:445–449.

Hayakawa, F., M. Towatari, H. Kiyoi, M. Tanimoto, T. Kitamura, H. Saito, and T. Naoe. 2000. Tandem-duplicated Flt3 constitutively activates STAT5 and MAP kinase and introduces autonomous cell growth in IL-3-dependent cell lines. *Oncogene.* 19:624–631.

Hirose, K., T. Kawashima, I. Iwamoto, T. Nosaka, and T. Kitamura. 2001. MgcRacGAP is involved in cytokinesis through associating with mitotic spindle and midbody. *J. Biol. Chem.* 276:5821–5828.

Ihle, J.N. 1996. Janus kinases in cytokine signalling. *Philos. Trans. R. Soc. Lond. B Biol. Sci.* 351:159–166.

Jantsch-Plunger, V., P. Gonczy, A. Romano, H. Schnabel, D. Hamill, R. Schnabel, A.A. Hyman, and M. Glotzer. 2000. CYK-4: a Rho family GTPase activating protein (GAP) required for central spindle formation and cytokinesis. *J. Cell Biol.* 149:1391–1404.

Kawashima, T., K. Hirose, T. Satoh, A. Kaneko, Y. Ikeda, Y. Kaziro, T. Nosaka, and T. Kitamura. 2000. MgcRacGAP is involved in the control of growth and differentiation of hematopoietic cells. *Blood.* 96:2116–2124.

Kawashima, T., K. Murata, S. Akira, Y. Tonozuka, Y. Minoshima, S. Feng, H. Kumagai, H. Tsuruga, Y. Ikeda, S. Asano, et al. 2001. STAT5 induces macrophage differentiation of M1 leukemia cells through activation of IL-6 production mediated by NF-kappaB p65. *J. Immunol.* 167:3652–3660.

Kutay, U., E.I. Izaurralde, F.R. Bischoff, I.W. Mattaj, and D. Görlich. 1997. Dominant-negative mutants of importin-β block multiple pathways of import and export through the nuclear pore complex. *EMBO J.* 16:1153–1163.

Lanning, C.C., R. Ruiz-Velasco, and C.L. Williams. 2003. Novel mechanism of the co-regulation of nuclear transport of SmgGDS and Rac1. *J. Biol. Chem.* 278:12495–12506.

Liu, L., K.M. McBride, and N.C. Reich. 2005. STAT3 nuclear import is independent of tyrosine phosphorylation and mediated by importin-alpha3. *Proc. Natl. Acad. Sci. USA.* 102:8150–8155.

Ma, J., and X. Cao. 2006. Regulation of Stat3 nuclear import by importin alpha5 and importin alpha7 via two different functional sequence elements. *Cell. Signal.* 18:1117–1126.

Marg, A., Y. Shan, T. Meyer, T. Meissner, M. Brandenburg, and U. Vinkemeier. 2004. Nucleocytoplasmic shuttling by nucleoporins Nup153 and Nup214 and CRM1-dependent nuclear export control the subcellular distribution of latent Stat1. *J. Cell Biol.* 165:823–833.

McBride, K.M., G. Banninger, C. McDonald, and N.C. Reich. 2002. Regulated nuclear import of the STAT1 transcription factor by direct binding of importin-α. *EMBO J.* 21:1754–1763.

Minoshima, Y., T. Kawashima, K. Hirose, Y. Tonozuka, A. Kawajiri, Y.C. Bao, X. Deng, M. Tatsuka, S. Narumiya, W.S. May Jr., et al. 2003. Phosphorylation by aurora B converts MgcRacGAP to a RhoGAP during cytokinesis. *Dev. Cell.* 4:549–560.

Mishima, M., S. Kaitna, and M. Glotzer. 2002. Central spindle assembly and cytokinesis require a kinesin-like protein/RhoGAP complex with microtubule bundling activity. *Dev. Cell.* 2:41–54.

Mizuki, M., R. Fenski, H. Halfter, I. Matsumura, R. Schmidt, C. Muller, W. Gruning, K. Kratz-Albers, S. Serve, C. Steur, et al. 2000. Flt3 mutations from patients with acute myeloid leukemia induce transformation of 32D cells mediated by the Ras and STAT5 pathways. *Blood.* 96:3907–3914.

Morita, S., T. Kojima, and T. Kitamura. 2000. Plat-E: an efficient and stable system for transient packaging of retroviruses. *Gene Ther.* 7:1063–1066.

Murata, K., H. Kumagai, T. Kawashima, K. Tamitsu, M. Irie, H. Nakajima, S. Suzu, M. Shibuya, S. Kamihira, T. Nosaka, et al. 2003. Selective cytotoxic mechanism of GTP-14564, a novel tyrosine kinase inhibitor in leukemia cells expressing a constitutively active Fms-like tyrosine kinase 3 (FLT3). *J. Biol. Chem.* 278:32892–32898.

Nakamura, T., R. Ouchida, T. Kodama, T. Kawashima, Y. Makino, N. Yoshikawa, S. Watanabe, C. Morimoto, T. Kitamura, and H. Tanaka. 2002. Cytokine receptor common beta subunit-mediated STAT5 activation confers NF-kappa B activation in murine proB cell line Ba/F3 cells. *J. Biol. Chem.* 277:6254–6265.

Nosaka, T., T. Kawashima, K. Misawa, K. Ikuta, A.L. Mui, and T. Kitamura. 1999. STAT5 as a molecular regulator of proliferation, differentiation and apoptosis in hematopoietic cells. *EMBO J.* 18:4754–4765.

Onishi, M., T. Nosaka, K. Misawa, A.L. Mui, D. Gorman, M. McMahon, A. Miyajima, and T. Kitamura. 1998. Identification and characterization of a constitutively active STAT5 mutant that promotes cell proliferation. *Mol. Cell. Biol.* 18:3871–3879.

Park, E.J., K.A. Ji, S.B. Jeon, W.H. Choi, I.O. Han, H.J. You, J.H. Kim, I. Jou, and E.H. Joe. 2004. Rac1 contributes to maximal activation of STAT1 and STAT3 in IFN-gamma-stimulated rat astrocytes. *J. Immunol.* 173:5697–5703.

Peifer, M., S. Berg, and A.B. Reynolds. 1994. A repeating amino acid motif shared by proteins with diverse cellular roles. *Cell.* 76:789–791.

Quelle, F.W., W. Thierfelder, B.A. Witthuhn, B. Tang, S. Cohen, and J.N. Ihle. 1995. Phosphorylation and activation of the DNA binding activity of purified Stat1 by the Janus protein-tyrosine kinases and the epidermal growth factor receptor. *J. Biol. Chem.* 270:20775–20780.

Ridley, A.J. 1995. Rho-related proteins: actin cytoskeleton and cell cycle. *Curr. Opin. Genet. Dev.* 5:24–30.

Roberts, A.W., C. Kim, L. Zhen, J.B. Lowe, R. Kapur, B. Petryniak, A. Spaetti, J.D. Pollock, J.B. Borneo, G.B. Bradford, et al. 1999. Deficiency of the hematopoietic cell-specific Rho family GTPase Rac2 is characterized by abnormalities in neutrophil function and host defense. *Immunity.* 10:183–196.

Saharinen, P., K. Takaluoma, and O. Silvennoinen. 2000. Regulation of the Jak2 tyrosine kinase by its pseudokinase domain. *Mol. Cell. Biol.* 20:3387–3395.

Sekimoto, T., N. Imamoto, K. Nakajima, T. Hirano, and Y. Yoneda. 1997. Extracellular signal-dependent nuclear import of Stat1 is mediated by nuclear pore-targeting complex formation with NPI-1, but not Rch1. *EMBO J.* 16:7067–7077.

Simon, A.R., H.G. Vikis, S. Stewart, B.L. Fanburg, B.H. Cochran, and K. Guan. 2000. Regulation of STAT3 by direct binding to the Rac1 GTPase. *Science.* 290:144–147.

Tonozuka, Y., Y. Minoshima, Y.C. Bao, Y. Moon, Y. Tsubono, T. Hatori, H. Nakajima, T. Nosaka, T. Kawashima, and T. Kitamura. 2004. A GTPase activating protein binds STAT3 and is required for IL-6-induced STAT3 activation and for differentiation of a leukemic cell line. *Blood.* 104:3550–3557.

Ushijima, R., N. Sakaguchi, A. Kano, A. Maruyama, Y. Miyamoto, T. Sekimoto, Y. Yoneda, K. Ogino, and T. Tachibana. 2005. Extracellular signal-dependent nuclear import of STAT3 is mediated by various importin alphas. *Biochem. Biophys. Res. Commun.* 330:880–886.

Van de Putte, T., A. Zwijsen, O. Lonnoy, V. Rybin, M. Cozijnsen, A. Francis, V. Baekelandt, C.A. Kozak, M. Zerial, and D. Huylebroeck. 2001. Mice with a homozygous gene trap vector insertion in mgcRacGAP die during pre-implantation development. *Mech. Dev.* 102:33–44.

Williams, C.C., J.G. Allison, G.A. Vidal, M.E. Burow, B.S. Beckman, L. Marrero, and F.E. Jones. 2004. The ERBB4/HER4 receptor tyrosine kinase regulates gene expression by functioning as a STAT5A nuclear chaperone. *J. Cell Biol.* 167:469–478.

Williams, D.A., W. Tao, F. Yang, C. Kim, Y. Gu, P. Mansfield, J.E. Levine, B. Petryniak, C.W. Derrow, C. Harris, et al. 2000. Dominant negative mutation of the hematopoietic-specific Rho GTPase, Rac2, is associated with a human phagocyte immunodeficiency. *Blood.* 96:1646–1654.

Yokota, S., H. Kiyoi, M. Nakao, T. Iwai, S. Misawa, T. Okuda, Y. Sonoda, T. Abe, K. Kahsima, Y. Matsuo, and T. Naoe. 1997. Internal tandem duplication of the FLT3 gene is preferentially seen in acute myeloid leukemia and myelodysplastic syndrome among various hematological malignancies. A study on a large series of patients and cell lines. *Leukemia.* 11:1605–1609.

Zeng, R., Y. Aoki, M. Yoshida, K. Arai, and S. Watanabe. 2002. Stat5B shuttles between cytoplasm and nucleus in a cytokine-dependent and -independent manner. *J. Immunol.* 168:4567–4575.

Zhang, S., S. Fukuda, Y. Lee, G. Hangoc, S. Cooper, R. Spolski, W.J. Leonard, and H.E. Broxmeyer. 2000. Essential role of signal transducer and activator of transcription (Stat)5a but not Stat5b for Flt3-dependent signaling. *J. Exp. Med.* 192:719–728.

Leukemia (2007) 21, 2246–2257

www.nature.com/leu

ORIGINAL ARTICLE

Identification of TSC-22 as a potential tumor suppressor that is upregulated by Flt3-D835V but not Flt3-ITD

Y Lu[1], J Kitaura[1], T Oki[1], Y Komeno[1], K Ozaki[1], M Kiyono[1], H Kumagai[1], H Nakajima[1], T Nosaka[1], H Aburatani[2] and T Kitamura[1]

[1]*Divisions of Cellular Therapy, Advanced Clinical Research Center, Institute of Medical Science, The University of Tokyo, Tokyo, Japan and* [2]*Genome Science Division, Research Center for Advanced Science and Technology, The University of Tokyo, Tokyo, Japan*

Transforming growth factor-β (TGF-β)-stimulated clone-22 (TSC-22) was originally isolated as a TGF-β-inducible gene. In this study, we identified TSC-22 as a potential leukemia suppressor. Two types of FMS-like tyrosine kinase-3 (Flt3) mutations are frequently found in acute myeloid leukemia: Flt3-ITD harboring an internal tandem duplication in the juxtamembrane domain associated with poor prognosis and Flt3-TKD harboring a point mutation in the kinase domain. Comparison of gene expression profiles between Flt3-ITD- and Flt3-TKD-transduced Ba/F3 cells revealed that constitutive activation of Flt3 by Flt3-TKD, but not Flt3-ITD, upregulated the expression of TSC-22. Importantly, treatment with an Flt3 inhibitor PKC412 or an Flt3 small interfering RNA decreased the expression level of TSC-22 in Flt3-TKD-transduced cells. Forced expression of TSC-22 suppressed the growth and accelerated the differentiation of several leukemia cell lines into monocytes, in particular, in combination with differentiation-inducing reagents. On the other hand, a dominant-negative form of TSC-22 accelerated the growth of Flt3-TKD-transduced 32Dcl.3 cells. Collectively, these results suggest that TSC-22 is a possible target of leukemia therapy.
Leukemia (2007) **21**, 2246–2257; doi:10.1038/sj.leu.2404883; published online 9 August 2007
Keywords: TSC-22; Flt3; AML

Introduction

Fms-like tyrosine kinase 3 (Flt3), originally isolated as a hematopoietic progenitor cell-specific kinase, belongs to the class III receptor tyrosine kinase family.[1,2] Flt3 is mainly expressed by early myeloid and lymphoid cells and has a crucial role in normal hematopoiesis,[1–5] while Flt3 mutations are frequently observed in acute myeloid leukemia (AML).[4,6,7] An internal tandem duplication within the juxtamembrane domain of the Flt3 gene (Flt3-ITD) or an activating mutation at aspartic acid 835 (D835) in the kinase domain of Flt3 (Flt3-D835), including Flt3-D835V, was found in 20–30 or 7%, respectively, of patients with AML.[8–16]

Whereas both types of Flt3 mutations cause constitutive activation of Flt3, resulting in autonomous proliferation of factor-dependent hematopoietic cell lines,[17–19] only Flt3-ITD was associated with poor clinical outcomes in both pediatric and adult patients with AML.[8,12,13,16,20–23] Recent accumulated data have shown that Flt3-ITD causes the constitutive activation of both Ras/extracellular regulated kinase (ERK) and signal transducer and activator of transcription 5 (STAT5), and that the activation of STAT5 is more prominent in the signaling pathway downstream of Flt3-ITD as compared with Flt3-D835.[18,24,25] However, the reason why Flt3-ITD causes poor clinical outcomes is not fully understood.

Transforming growth factor-β (TGF-β)-stimulated clone-22 (TSC-22) was initially isolated from mouse osteoblastic cells as an immediate early response gene of TGF-β.[26] It encodes a putative transcriptional regulator containing a leucine zipper structure that is highly conserved between many species.[26–30] TSC-22 was upregulated by many different stimuli such as anticancer drugs[29] and a variety of growth factors and cytokines, including follicle-stimulating hormone,[30] fibroblast growth factor-2,[31] progesterone,[32] epidermal growth factor,[33] TGF-β,[26,27,29] tumor necrosis factor-α, interferon-γ and interleukin-1β.[27] TSC-22 was also expressed in a dynamic pattern at sites of epithelial–mesenchymal interactions during mouse development.[34,35] Accumulated data suggest that TSC-22 is a potential tumor suppressor gene, because TSC-22 was a progesterone target gene upregulated in breast cancer cells, where growth is inhibited by progestins.[32] In addition, overexpression of the TSC-22 gene caused apoptotic cell death involved in the activation of caspase-3 in a human gastric carcinoma cell line[36] and TSC-22 suppressed growth in a salivary gland carcinoma cell line and reduced tumor formation in nude mice.[29,37,38]

In this study, to understand the molecular basis for the fact that Flt3-ITD, but not Flt3-TKD, is associated with poor prognosis, we transduced Flt3-ITD and Flt3-D835V into a mouse IL-3-dependent pro-B cell line Ba/F3 and compared the gene expression profiles downstream of Flt3-ITD and Flt3-D835V. We identified TSC-22 as a gene upregulated by Flt3-D835V, but not by Flt3-ITD. We report the effect of TSC-22 on the proliferation and differentiation of leukemia cells in the context of leukemic therapy.

Materials and methods

Reagents

Recombinant murine interleukin-3 (rmIL-3), recombinant human Flt3 ligand (rhFL), and recombinant murine granulocyte colony-stimulating factor (G-CSF) were obtained from R&D Systems (Minneapolis, MN, USA). Mouse anti-human CD14 and anti-human leukocyte antigen-DR (HLA-DR) monoclonal antibodies (mAbs) were purchased from Becton Dickinson (San Jose, CA, USA). Mouse anti-human CD80 mAb were from ImmunoTech Co., Ltd (Osaka, Japan). Phycoerythrin (PE)-labeled mouse anti-human Flt3 (CD135) and CD11b mAbs were from BD Pharmingen (San Diego, CA, USA). Rabbit

Correspondence: Dr T Kitamura, Division of Cellular Therapy, Advanced Clinical Research, Institute of Medical Science, University of Tokyo, 4-6-1 Shirokanedai, Minato-ku, Tokyo 108-8639, Japan.
E-mail: kitamura@ims.u-tokyo.ac.jp
Received 15 September 2006; revised 23 June 2007; accepted 26 June 2007; published online 9 August 2007

polyclonal anti-ERK-1/2 antibody (Ab) was from Cell Signaling Technology (Beverly, MA, USA). Rabbit polyclonal anti-Flt3 Ab was from Santa Cruz Biotechnology (Santa Cruz, CA, USA). PKC412 was obtained from Novartis Pharmaceuticals (Basel, Switzerland). 12-*O*-tetradecyanoylphorbol 13-acetate (PMA) and 1,25-dihydroxy vitamin D3 (Vit.D3) were from Sigma (St Louis, MO, USA). Fibrinogen (FB) was from Calbiochem (San Diego, CA, USA).

Cell lines and cell culture

The murine pro-B cell line, Ba/F3 cells and the murine myeloid progenitor cell line, 32Dcl.3 (32D) cells were maintained in RPMI 1640 containing 10% fetal calf serum (FCS), penicillin/streptomycin and 1 ng/ml rmIL-3. The murine B-cell lymphoma line, WEHI-231 (WEHI) cells were cultured in RPMI 1640 containing 10% FCS, 50 mM 2-mercaptoethanol and penicillin/streptomycin. The human leukemia cell lines, U937 and HL-60 cells, were maintained in RPMI 1640 containing 10% FCS, penicillin/streptomycin. An ecotropic retrovirus packaging cell line, Plat-E cells, was maintained in Dulbecco's modified Eagle's medium containing 10% FCS, 1 μg/ml puromycin (Sigma) and 10 μg/ml blasticidin S (Funakoshi Co., Tokyo, Japan).

DNA constructs and retroviral transfection

The construction of pMKIT-Neo vectors containing Flt3-wild type (WT) or Flt3-ITD and the transfection of Ba/F3 cells with these vectors were described previously.[39] The Flt3-D835V and Flt3-D835Y constructs were amplified by two-step polymerase chain reaction (PCR) from Flt3-WT in pMKIT-Neo vector using PFU DNA polymerase (Stratagene, La Jolla, CA, USA). Primers used in step 1 were: forward Flt3-*Bam*HI: 5′-CGCGGATCCATG GGCCCAGGAGTTCTG-3′, reverse Flt3-D835V: 5′-CATGATAA CGCGTGCCAATTCAAA-3′ or reverse Flt3-D835Y: 5′-GAATCA CTCATGATATATCGAGC-3′. Primers used in step 2 were: forward Flt3-D835V: 5′-TTTGGATTGGCACGCGTTATCATG-3′ or forward Flt3-D835Y: 5′-GCTCGATATATCATGAGTGATTC-3′, reverse Flt3-*Xba*I: 5′-GCTCTAGACTACGAATCTTCGACC TG-3′. PCR products from step 1 and step 2 were diluted and combined as templates using Flt3-*Bam*HI and Flt3-*Xba*I as the forward or reverse primers, respectively, to create mutant fragments, which were then subcloned into the pMKIT-Neo expression vector. For generation of stably transfected 32D cells, the sequence of Flt3-WT, Flt3-ITD, Flt3-D835V or Flt3-D835Y excised from pMKIT-Neo was subcloned into pMXs-IERS-Neomycin (pMXs-IN) retroviral vector.[40] The Plat-E packaging cells were transfected with these vectors by FuGENE 6 transfection reagent (Roche Diagnostics, Indianapolis, IN, USA) as described previously.[40] The retroviruses were used to infect 32D cells in the presence of rmIL-3. Stable transfectants were then selected with 1 mg/ml G418 (Nacalai Tesque Inc., Kyoto, Japan) for 2 weeks. Ba/F3 and 32D transfectants expressing Flt3-ITD, Flt3-D835V or Flt3-D835Y were maintained in RPMI 1640 containing 10% FCS in the absence of rmIL-3, while Flt3-WT-expressing cells were maintained in the presence of 10 ng/ml rhFL. The coding sequence of mouse TSC-22 was amplified by PCR from complementary DNA (cDNA) of Ba/F3 cells using AmpliTaq Gold (Roche Molecular Systems Inc., Branchburg, NJ, USA) and subcloned into pMXs-IERS-Puromycin (pMXs-IP) retroviral vectors.[40] A truncated TSC-22-LZ was amplified by PCR from plasmid, pEGFP-TSC-22-LZ (kindly provided by Hitoshi Kawamata, School of Medicine, Dokkyo University, Japan) and subcloned into pMXs-IP retroviral vectors. TSC-22-LZ contains TSC-box and leucine zipper, but not both repressor domains (RD). For retroviral transduction of TSC-22 into Ba/F3, 32D, WEHI, U937, HL-60 cells or Flt3-ITD-expressing cells, Plat-E packaging cells were transfected with pMXs-IP, pMXs-TSC-22-IP or pMXs-TSC-22-LZ-IP construct before infection with retroviruses. To avoid clonal differences as well as a bias by the selection in the absence of IL-3, pooled transfectants were selected with 2 μg/ml puromycin for 2 weeks and were subjected to experiments. These procedures were performed multiple times with the similar results.

Microarray analysis

Ba/F3 transfectants expressing Flt3-ITD or Flt3-D835V were maintained in the absence of rmIL-3. Total RNA was extracted by Trizol reagent (Invitrogen, Carlsbad, CA, USA) according to the manufacturer's protocol. Double-stranded cDNA was synthesized from 5 μg of total RNA with oligo $(dT)_{24}$ T7 primer, amplified with T7 RNA polymerase up to approximately 50 μg of cRNA, and hybridized to Affymetrix Mouse Expression array 430A, which contains 45 000 probe sets for 39 000 transcripts and variants from over 34 000 well-characterized mouse genes (Affymetrix, Santa Clara, CA, USA). After washing and staining, the arrays were scanned on the GeneChip system confocal scanner (Affymetrix, Hewlett-Packard, Santa Clara, CA, USA). The intensity for each feature of the array was captured with Affymetrix Microarray Suite (MAS) Version 5.0 software.

Real-time reverse transcription-PCR

Real-time reverse transcription-PCR was performed using a LightCycler Workflow System (Roche Diagnostics, Mannheim, Germany). cDNA was synthesized and amplified from 200 ng of RNA using a LightCycler FastStart DNA Master SYBR Green I kit (Roche Diagnostics). Reaction was subject to 45 cycles of PCR at 95°C for 10 s, 55°C for 10 s and 72°C for 20 s. All samples were independently analyzed at least three times. The following primer pairs were used: 5′-ATGAAATCCCAATGGTGTAGA-3′ (TSC-22 forward), 5′-CTATGCGGTTGATCCTGAGCC-3′ (TSC-22 reverse). The housekeeping gene, glyceraldehyde-3-phosphate dehydrogenase (GAPDH), served as an additional control for cDNA quality. Relative gene expression levels were calculated using standard curves generated by serial dilutions of cDNA of Ba/F3 cells or 32D cells. Product quality was checked by melting curve analysis via LightCycler software (Roche Diagnostics). Expression levels for each gene were divided by the GAPDH RNA expression level.

siRNA transfection

An Flt3-specific SMARTPool and Nonspecific control small interfering RNA (siRNA) were purchased from Dharmacon (Lafayette, CO, USA). For transfection, 5×10^6 cells were resuspended in the specific Nucleofector Solution V, mixed with 2.5 μg double-stranded siRNA targeting Flt3 mRNA or control siRNA, and nucleofected with the cell-specific program X-001 using the Amaxa Nucleofector Device (Amaxa, Gaithersburg, MD, USA), according to the manufacturer's protocols. Cells were analyzed 24 h after transfection by western blot and flow cytometry analysis.

Generation of anti-TSC-22 antibody

Purification of recombinant TSC-22 protein and generation of anti-TSC-22 polyclonal antibody was performed as described previously.[37] Briefly, a cDNA for the mouse TSC-22 was subcloned in the correct reading frame into pGEX4T-1

(Amersham Biosciences, Uppsala, Sweden) and verified by sequencing. glutathione *S*-transferase (GST)–TSC-22 was expressed in *Escherichia coli* strain BL21 (DE3) cultured with 100 mM lactose analog isopropylβ-D-thiogalactoside. GST-fusion proteins were purified by glutathione-sepharose 4B according to the standard protocols (Amersham Biosciences). Anti-TSC-22 polyclonal antibody was generated from the serum of immunized rabbit using purified GST–TSC-22 fusion protein (SCRUM Inc., Tokyo, Japan). In western blot analysis, this antibody detected two bands, the large of which corresponded to the full-length protein in size.

Immunoprecipitation and western blot analysis

Cells were lysed in lysis buffer (10% glycerol, 150 mM NaCl, 50 mM Tris-HCl at pH7.5, 1% NP-40) containing protease and phosphatase inhibitor cocktail tablets (Sigma), and then cell lysates were clarified by centrifugation. The protein concentration of the supernatants was determined with a Bio-Rad Protein Assay kit (Rio-Rad, Hercules, CA, USA). For immunoprecipitation, equivalent amounts of protein were incubated with anti-TSC-22 antibody and protein G Sepharose at 4°C for 2 h. The immunoprecipitates were washed four times with lysis buffer, then resuspended in sodium dodecyl sulfate (SDS) sample buffer and heated at 95°C for 5 min. Cell lysates or immunoprecipitates were separated by SDS-polyacrylamide gel electrophoresis gel (Wako, Osaka, Japan). Gels were transferred onto Immobilon membranes (Millpore, Bedford, MA, USA) and immunostained with an anti-TSC-22 Ab, anti-Flt3 Ab or anti-ERK Ab, followed by a horseradish peroxidase-labeled secondary Ab. Stained protein was visualized by chemiluminescence using ECL reagents (Amersham Biosciences).

Flow cytometry

Cells were washed with phosphate-buffered saline (PBS)/2% FCS, blocked with mouse FcBlock (BD Biosciences, Franklin Lakes, NJ, USA) for 15 min, and stained with the indicated antibodies for 20 min. After washing, cells were analyzed using a FACSCalibur flow cytometer with CellQuest software (BD Biosciences).

Analysis of cell growth

The cells were resuspended in RPMI 1640 including 10% FCS with or without indicated growth factors, and 1×10^3 cells were seeded into 96-well plates (Corning, NY, USA). After incubation for the indicated time at 37°C, cell growth was estimated by quantitating luminescence from the 96-well plates using CellTiter-Glo (Promega, Madison, WI, USA) and a Micro Lumat Plus luminometer (EG&G Berthold), according to the manufacturer's instructions. Briefly, the luminescence is recorded with a luminometer measuring the amount of ATP which is proportional to viable cell number.

Adhesion assay

Adhesion assay was performed as described previously.[41] In brief, the 96-well plates (Corning) were coated with 20 μg/ml FB in PBS for 1 h at 37°C, washed three times with PBS, blocked with 3% bovine serum albumin (BSA)/PBS for 1 h at 37°C, and washed three times with RPMI 1640. Cells were resuspended with the RPMI 1640 containing 10% FCS and transferred into coated wells with or without 1 ng/ml rmIL-3. The plates were incubated at 37°C for 2 h, and the unbound cells were washed away. Input and bound luminescence were directly quantitated from the 96-well plates using CellTiter-Glo and a Micro Lumat Plus luminometer. The percent of adhesion was calculated by dividing bound luminescence by input luminescence.

The evaluation of cell differentiation

U937 and HL-60 cells were seeded at 3×10^5 cells/ml and treated with 10 ng/ml PMA or 10 nM Vit.D3 for the indicated time. Surface expression level of CD11b, CD14, CD80 or HLA-DR was estimated by flow cytometry. Cells of cytocentrifuged by Shandon Cytopsin (Thermo Fisher SCIENTIFIC, Waltham, MA, USA) were stained with May-Grunwald-Giemsa and evaluated morphologically.

Mice

Eight-week-old male Balb/c mice or C3H/HeJ mice were purchased from Charles River Japan Inc. Mice were kept under standard laboratory conditions according to the guidelines of the Laboratory Animal Research Center, The Institute of Medical Science, The University of Tokyo. The transduced Ba/F3 cells (1×10^6 cells) or 32D cells (1×10^5 cells) were injected into the lateral tail vein of Balb/c or syngeneic C3H/HeJ mice, respectively. The injected mice (five mice in each group) were monitored daily. This study was approved by the Institutional Ethics Committee for Laboratory Animals Used in Experimental Research.

Statistical analysis

Statistical significance was calculated using the Student *t*-test for independent variables with Excel (Microsoft). *P*-values < 0.05 were considered statistically significant.

Results

Leukemia-like disease was rapidly induced by Flt3-ITD-transduced Ba/F3 cells but not by Flt3-D835V-transduced Ba/F3 cells

As reported, both Flt3-ITD and Flt3-TKD led to factor-independent growth of the transduced Ba/F3 cells.[9,14,15,17] We next investigated the leukemogenic potential of the transduced Ba/F3 cells by injecting them into syngeneic Balb/c mice. All the mice receiving the Flt3-ITD-transduced cells developed a lethal hematopoietic disease with a median latency period of approximately 8–9 weeks (Figure 1a). In contrast, only four of 10 mice receiving the Flt3-D835V-transduced cells developed a similar disease, with a longer latency period of 10–12 weeks. The remaining six mice were as healthy as the mice given an injection of the Flt3-WT-transduced cells during an extended observation time of 120 days. Histopathological analysis of the mice inoculated with Flt3-ITD-transduced cells revealed marked pathological findings. The expansion and infiltration of leukemia-like cells observed in liver and bone marrow confirmed the strong transforming ability of the Ba/F3 cells expressing Flt3-ITD (data not shown).

TSC-22 is highly expressed in Flt3-TKD-transduced cells but not in Flt3-ITD-transduced cells

The different phenotypes observed in transplantation experiments using the Flt3-ITD- or Flt3-D835V-transduced Ba/F3 cells prompted us to investigate the underlying molecular mechanisms. We hypothesized that the changes in gene expression patterns induced by Flt3-ITD or Flt3-D835V might reflect the

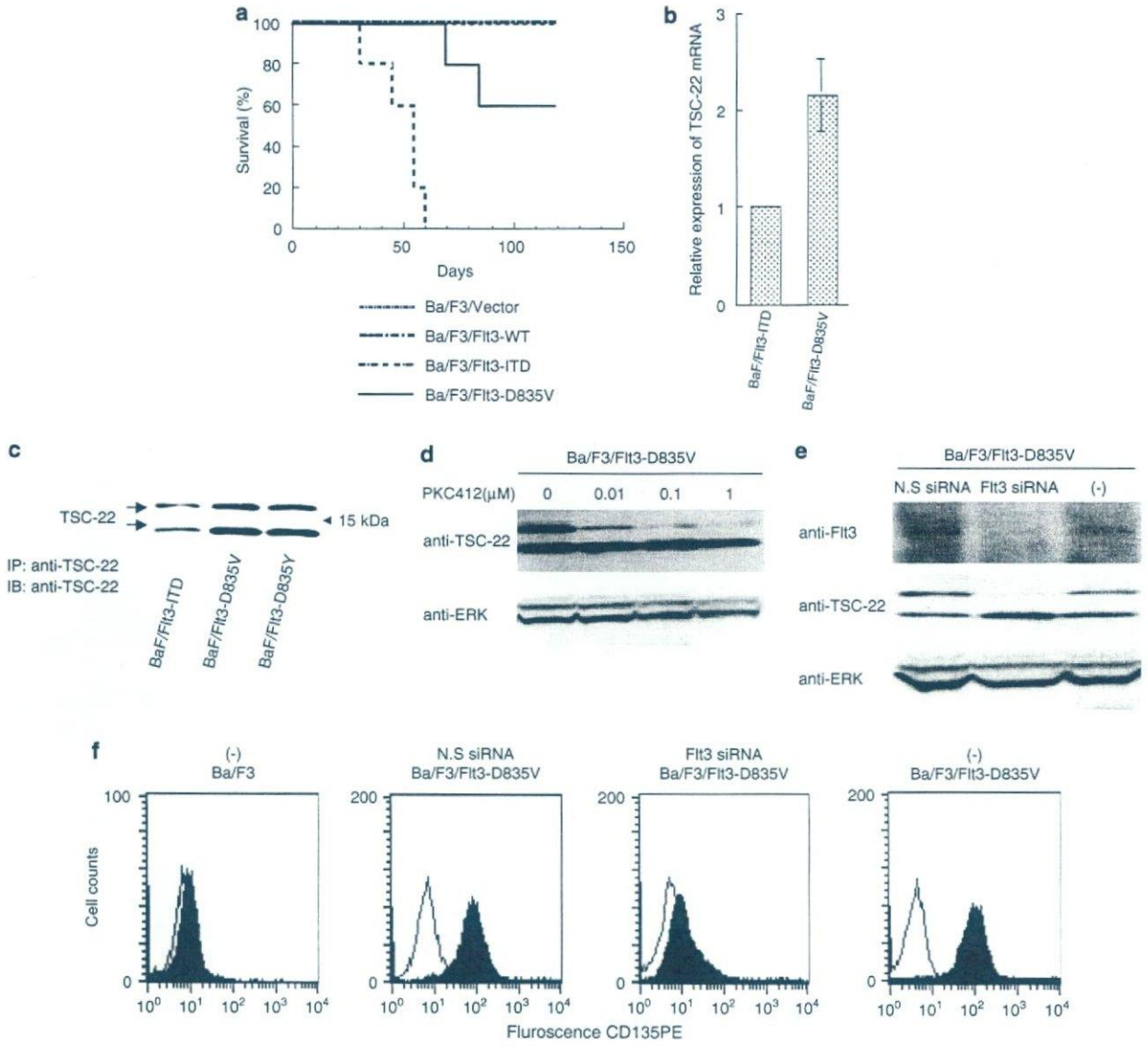

Figure 1 *In vivo* and *in vitro* effects of Flt3-ITD and Flt3-D835V. (**a**) Kaplan–Meier plot of survival. Balb/c mice ($n = 5$ for each group) were injected via tail veins with 1×10^6 Ba/F3 cells expressing Flt3-WT, Flt3-ITD, Flt3-D835V and vector as control. Mouse survival was monitored daily for 120 days. The percentage of surviving mice (*y* axis) is plotted over the time after injection (*x* axis). This graph presents data from two independent experiments. (**b**) Quantification of TSC-22 mRNA levels in Ba/F3 cells by real-time RT-PCR. Total RNA was isolated from Ba/F3 transfectants under the same conditions as shown in Table 1. The bar represents the ratios of GAPDH-normalized expression values. Each bar represents the mean of three independent experiments. (**c**) Expression levels of TSC-22 protein in Ba/F3 transfectants. Equivalent amounts of cell extracts prepared from Ba/F3 transfectants were immunoprecipitated with anti-TSC-22 antibody, followed by immunoblotting with the same antibody. (**d**) Downregulation of TSC-22 by an Flt3 inhibitor PKC412. Flt3-D835V-expressing BaF3 cells were incubated with the indicated concentrations of PKC412 for 24 h in the absence of rmIL-3. Equivalent amounts of cell lysates were immunoblotted with anti-ERK Ab or immunoprecipitated with anti-TSC-22Ab, followed by immunoblotting with the same Ab. (**e–f**) Flt3 siRNA-induced downregulation of TSC-22. Flt3-D835V-expressing BaF3 cells were nucleofected with Flt3 or nonspecific control siRNA in the absence of rmIL-3. Expression of Flt3-D835V was determined (**e**) by immunoblotting of equivalent amounts of total cell lysates with anti-Flt3 Ab or (**f**) by flow cytometry analysis using isotype control mAb (blank areas) and PE-conjugated anti-CD135 mAb (filled areas) 24 h after siRNA transfection. Expression of TSC-22 or ERK was determined as described above. Ab, antibody; ERK, extracellular regulated kinase; GAPDH, glyceraldehyde-3-phosphate dehydrogenase; mAb, monoclonal antibody; PE, phycoerythrin; RT-PCR, reverse transcription-PCR; siRNA, small interfering RNA; TSC-22, TGF-β-stimulated clone-22.

different phenotypes during leukemogenesis. Therefore, we analyzed the gene expression profiles of Ba/F3 cells expressing Flt3-ITD or Flt3-D835V by microarray experiments. We chose the genes that were up- or downregulated at least twofold between the cells expressing Flt3-ITD versus Flt3-D835V (Table 1). Among them, we focused on one of the genes upregulated in Flt3-D835V-expressing cells, TSC-22, because it is known to be a tumor suppressor involved in the induction of apoptosis.

First, we quantified expression levels of TSC-22 mRNA by real-time PCR and confirmed that the Flt3-ITD-transduced Ba/F3 cells expressed a lower level of TSC-22 mRNA when compared with Flt3-D835V-transduced Ba/F3 cells (Figure 1b). Thus, the real-time PCR results were consistent with the microarray data

Table 1 Expression of genes regulated by Flt3-ITD and Flt3-D835V

Gene symbol	*Gene description*	*Average difference*	
		Flt3-ITD	*Flt3-D835V*
Increased by Flt3-ITD			
Ms4a3	Membrane-spanning 4-domains, subfamily A, member 3	204	100.4
Bnip3	BCL2/adenovirus E1B 19 kDa-interacting protein 1, NIP3	226.5	80.6
Cd47	CD47 antigen (Rh-related antigen, integrin-associated signal transducer)	248.3	105
Enh-pending	Enigma homolog (R. norvegicus)	265.2	107.6
Podxl	podocalyxin-like	303.9	142.4
Csf2rb1	Colony stimulating factor 2 receptor, beta 1, low-affinity (granulocyte-macrophage)	355.3	162.8
Hba-a1	Hemoglobin alpha, adult chain 1	423.1	150.2
Serpina3g	Serine (or cysteine) proteinase inhibitor, clade A, member 3G	475.3	49.7
Tcrg-V4	T-cell receptor gamma, variable 4	501.1	182.6
Cd53	CD53 antigen	549.3	268.2
Csf2rb2	Colony stimulating factor 2 receptor, beta 2, low-affinity (granulocyte-macrophage)	861.1	349.6
Decreased by Flt3-D835V			
Tgfb1i4 (TSC-22)	Transforming growth factor beta 1 induced transcript 4	124.5	279.2
Hbb-b1	Hemoglobin, beta adult major chain	288.7	817.9

Changes in gene expression in Ba/F3 cells expressing Flt3-ITD and Flt3-D835V. RNAs harvested from Ba/F3 transfectants without cytokines were hybridized to mouse expression array. Only genes with fold differences of raw data >2 are listed.

described above. Next, we examined whether the change in mRNA levels correlated with that in protein levels. Since Flt3-D835Y is most frequently found among Flt3-TKD mutations, we examined the expression levels of TSC-22 in the cell lysates prepared from Flt3-D835Y-expressing Ba/F3 cells in addition to Flt3-ITD- and Flt3-D835V-expressing Ba/F3 cells. Immunoprecipitated lysate with anti-TSC-22 Ab was subject to immunoblotting for TSC-22. As shown in Figure 1c, western blot analysis revealed higher expression of TSC-22 in Flt3-D835V- and Flt3-D835Y-expressing cells compared to that in Flt3-ITD-expressing cells. To explore whether the kinase activity of Flt3-TKD is required for upregulation of TSC-22, we treated Flt3-D835V-expressing Ba/F3 cells with increasing concentrations of a known Flt3 inhibitor PKC412 for 24 h in the absence of rmIL-3.[42] As shown in Figure 1d, PKC412 dose-dependently decreased protein expression levels of a full length of TSC-22, while it did not affect expression level of ERK1/2 used as a control. Moreover, to determine whether sufficient expression levels of Flt3-TKD is indispensable for upregulation of TSC-22, we performed experiments to downregulate Flt3-D835V by transfecting Flt3 siRNA into Flt3-D835V-expressing Ba/F3 cells.[43] Flt3 siRNA, but not control siRNA, strongly inhibited the expression of Flt3-D835V at protein levels 24 h after transfection, although it did not affect that of ERK1/2 (Figure 1e). At the same time, flow cytometry analysis clearly demonstrated a drastic reduction of surface expression levels of Flt3-D835V by Flt3 siRNA, but no by control siRNA (Figure 1f). Importantly, a full length of TSC-22 was strongly inhibited in accordance with downregulation of Flt3-D835 by siRNA (Figure 1e). Collectively, sufficient expression and kinase activity of Flt3-TKD was indispensable for upregulation of TSC-22.

To further confirm if these data generally applied to hematopoietic cell lines, another murine myeloid cell line, 32D, was stably transfected with either Flt3-WT, Flt3-ITD, Flt3-D835V or Flt3-D835Y construct. Flow cytometry analysis revealed that the surface expression levels of Flt3-ITD, Flt3-D835V and Flt3-D835Y were comparable, but slightly lower than that of Flt3-WT and higher than that of endogenous Flt3 (Figure 2a). Then, we analyzed TSC-22 expression at both mRNA and protein levels. In accordance with the data using Ba/F3 cells, the expression level of TSC-22 in Flt3-ITD-ransduced 32D cells was significantly lower than those of Flt3-D835V- and Flt3-D835Y-transduced 32D cells in the presence of rmIL-3 (Figures 2b and c). Then, we compared the growth of 32D cells carrying either Flt3-ITD, Flt3-D835V or Flt3-D835Y. As reported, Flt3-ITD-, Flt3-D835V- and Flt3-D835Y-transduced 32D cells proliferated independently of an exogenous growth factor IL-3, although Flt3-D835V- and Flt3-D835Y-expressing cells showed a weaker proliferative response than Flt3-ITD-expressing cells (Figure 2d). Taken together, while both Flt3-ITD and Flt3-TKD induced factor-independent growth of 32D cells, upregulation of TSC-22 expression was observed only in the cells transduced with Flt3-D835V and Flt3-D835Y but not those transduced with Flt3-ITD. We postulated that the lower expression levels of TSC-22 might be associated with the higher rate of cell proliferation, resulting in the rapid induction of leukemia-like disease by Flt3-ITD-carrying cells.

Forced expression of TSC-22 inhibits cell growth in several leukemia-derived cell lines

To further evaluate the effects of TSC-22 on cell proliferation, we transduced TSC-22 or its dominant-negative form TSC-22-LZ into several leukemia-derived cell lines, including 32D, WEHI or U937 cells. TSC-22-LZ containing TSC-box and leucine zipper but not two RD has been reported to act as a dominant-negative inhibitor.[44] Flow cytometry analysis revealed that the surface expression levels of transduced-Flt3 isoforms were not altered with or without transduced-TSC-22 in 32D cells (Figure 3a). Enforced expression of TSC-22 or TSC-22LZ was confirmed by western blot using an anti-TSC-22 mAb (data not shown). As shown in Figure 3b (left panel), IL-3-dependent growth of 32D cells was significantly inhibited or accelerated by exogenous expression of TSC-22 or TSC-22-LZ, respectively. Interestingly, autonomous growth of Flt3-ITD-transduced 32D cells was significantly inhibited by exogenous expression of TSC-22 as shown in Figure 3b (right panel), while growth of Flt3-TKD-transduced 32D cells was accelerated by forced expression of TSC-22-LZ as shown in Figure 3d. Intriguingly, enforced expression of TSC-22 significantly inhibited the growth of Flt3-ITD-expressing cells down to the growth rate of Flt3-D835V-expressing cells (Figure 3e). We also demonstrated similar effects of TSC-22 on the growth of WEHI and U937 cells (Figure 3c). To next examine the *in vivo* effect of TSC-22 on the

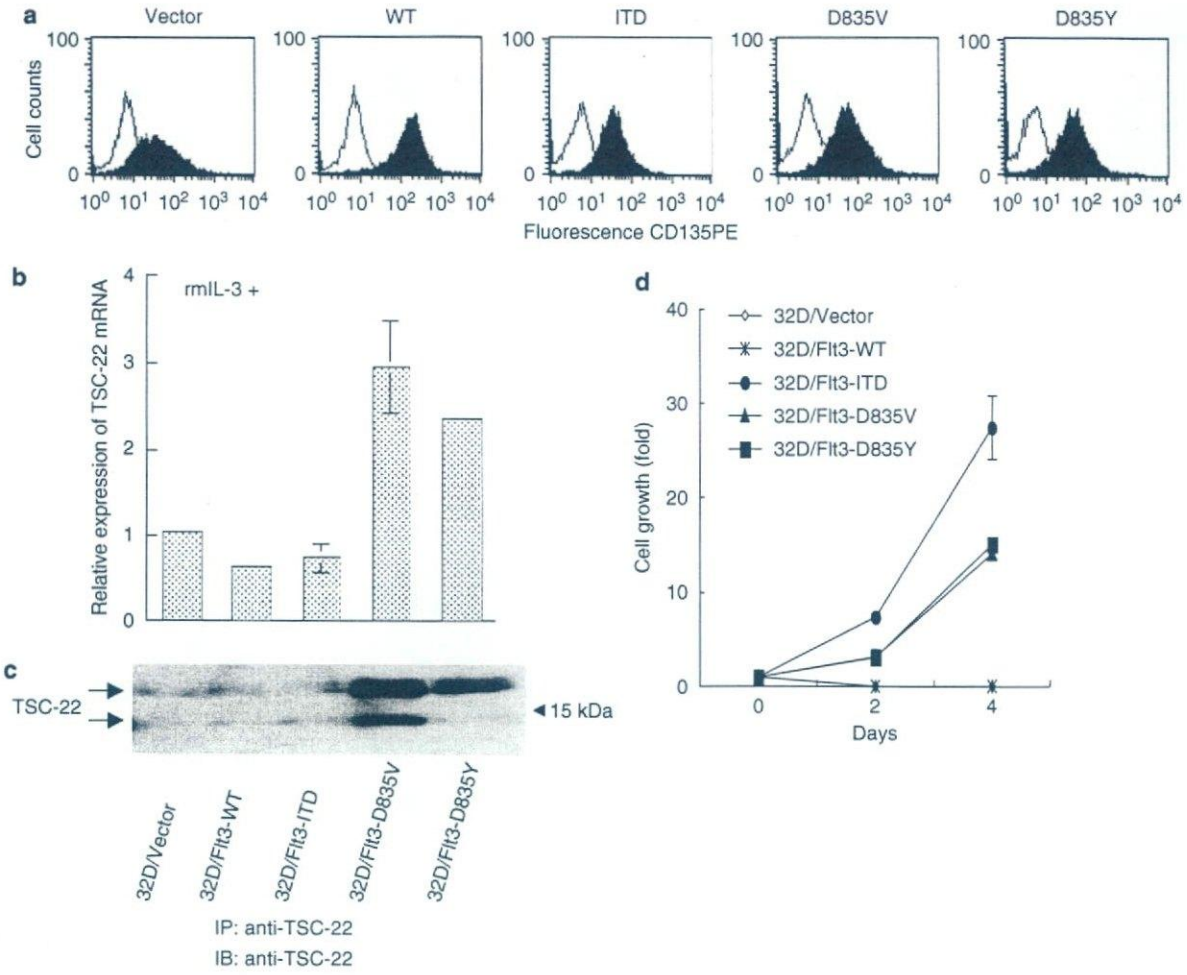

Figure 2 TSC-22 was upregulated by Flt3-TKD, but not by Flt3-ITD. (**a**) Surface expression of transduced Flt3 receptors. 32D cells infected with vector control, Flt3-WT, Flt3-ITD, Flt3-D835V and Flt3-D835Y viruses were stained with isotype control mAb (blank areas) and anti-PE-conjugated CD135 mAb (filled areas). (**b**) Quantification of TSC-22 mRNA levels in 32D cells by real-time RT-PCR. Total RNA was isolated from 32D transfectants cultured as indicated. The bar represents the ratios of GAPDH-normalized expression values. The mean of the expression levels in vector-plasmid transfected cells was set as 1. Each bar represents the mean of three independent experiments. (**c**) The expression levels of TSC-22 protein in 32D transfectants. Equivalent amounts of cell extracts prepared from 32D transfectants were immunoprecipitated with anti-TSC-22 antibody, followed by immunoblotting with the same antibody. (**d**) The growth of 32D transfectants. 32D cells infected with Vector, Flt3-WT, Flt3-ITD, Flt3-D835V or Flt3-D835Y viruses were seeded at a density of 1×10^4 cell/ml on 96-well plates in the absence of growth factor. Viable cells of triplicate cultures were quantitated by measuring luminescence using a Micro Lumat Plus luminometer at the indicated times. The means and s.d. are shown. GAPDH, glyceraldehyde-3-phosphate dehydrogenase; mAb, monoclonal antibody; PE, phycoerythrin; RT-PCR, reverse transcription-PCR; TSC-22, TGF-β-stimulated clone-22.

proliferation of leukemic cells, we injected Flt3-ITD-transduced 32D cells with or without enforced expression of TSC-22 into the C3H/HeJ mice. Overexpression of TSC-22 marginally extended the survival of C3H/HeJ mice inoculated with Flt3-ITD-transduced 32D cells (Figure 3f), suggesting attenuated growth of the leukemic cells by TSC-22. We concluded that enforced expression of TSC-22 led to decreased growth rates in several leukemia-derived cell lines.

32D cells acquire adhesive properties by forced expression of TSC-22

A differentiation block is one of the characteristics of leukemia cells. As previously reported by Zheng *et al.*,[45] 32D cells differentiated into mature granulocytes in the presence of G-CSF, while Flt3-ITD-expressing 32D cells did not. To examine whether TSC-22 was involved in the differentiation, we performed a similar experiment using Flt3-ITD-carrying 32D cells transfected with the TSC-22 construct. Forced expression of TSC-22 did not affect the differentiation into granulocytes in the presence or absence of G-CSF (data not shown). However, we found that parental or Flt3-ITD-carrying 32D cells adhered to the plastic plates by forced expression of TSC-22. To confirm this, an adhesion assay using BSA- or FB-coated plates was conducted. As shown in Figure 4a, the number of cells adhering to the plates was significantly increased by forced expression of TSC-22. The adherent cells displayed well-spread morphology, similar to monocytes/macrophages (Figure 4b). Expression levels of several integrins and surface markers indicative of granulocytes or monocytes/macrophages did not change except that CD11b expression level was slightly increased by the enforced expression of TSC-22 (data not shown). These results indicated that TSC-22 might play a role in the differentiation, giving an adhesive property to the cells.

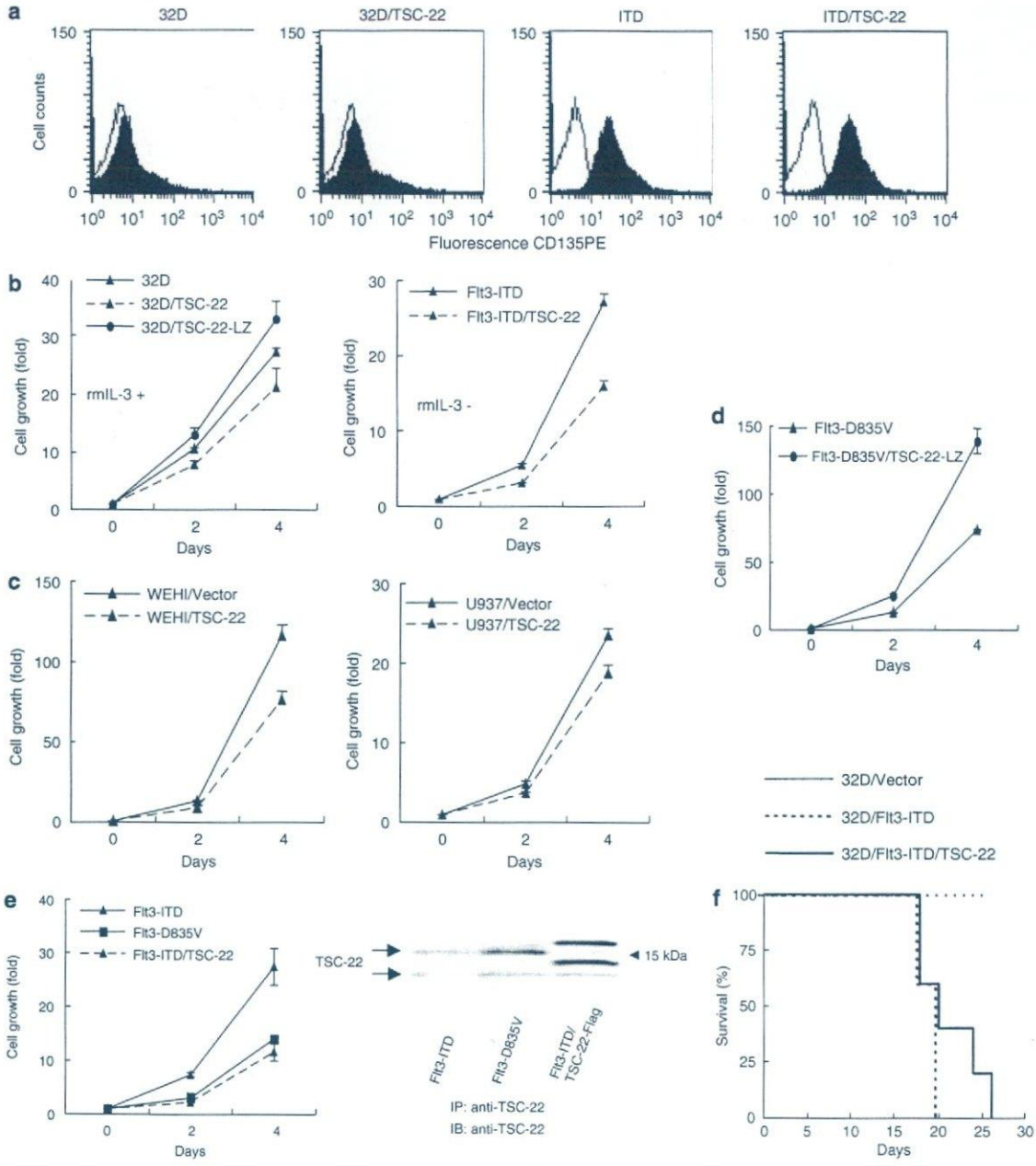

Figure 3 Forced expression of TSC-22 suppressed the proliferation of 32D, WEHI and U937 cells. (**a**) Surface expression of endogenous Flt3 and transduced Flt3-ITD. 32D or Flt3-ITD-transduced 32D cells were infected with TSC-22 or vector control viruses and stained with isotype control mAb (blank areas) and anti-PE-conjugated CD135 mAb (filled areas). (**b–d**) The growth of several cell transfectants. 32D, Flt3-ITD-transduced 32D cells infected with TSC-22, TSC-22-LZ or vector control viruses (**b**), WEHI, U937 cells infected with TSC-22 or empty vectors (**c**), and Flt3-D835V-transduced 32D cells infected with TSC-22-LZ or vector control viruses (**d**) were seeded at a density of 1×10^4 cell/ml into 96-well plates with or without growth factor. Viable cells of triplicate cultures were quantitated as described previously at the indicated times. The means and s.d. are shown. (**e**) Growth rates of the Flt3 transfectants. Flt3-ITD-, Flt3-D835V-transduced 32D cells and Flt3-ITD-expressing 32D cells co-transduced with TSC-22 were examined (left panel). Expression levels of endogenous and exogenous TSC-22 among these cells were determined as described above (right panel). (**f**) Kaplan–Meier plot of survival. C3H/HeJ mice ($n = 5$ in each group) were injected via tail vein with 1×10^5 of 32D cells expressing Flt3-ITD, Flt3-ITD/TSC-22 and vector as control. Mouse survival was monitored daily. The percentage of surviving mice (y axis) is plotted over the time after injection (x axis). This graph presents data from two independent experiments. mAb, monoclonal antibody; PE, phycoerythrin; TSC-22, TGF-β-stimulated clone-22.

Expression of TSC-22 promotes monocytic differentiation of several leukemia cells

To elucidate the role of TSC-22 in the differentiation of leukemia cells, we performed experiments using differentiation-inducing reagents. When U937 cells transfected with a TSC-22 construct or vector alone were exposed to 10 ng/ml PMA, both TSC-22-transduced and control U937 cells showed decreased proliferation. However, TSC-22-carrying U937 cells treated with PMA

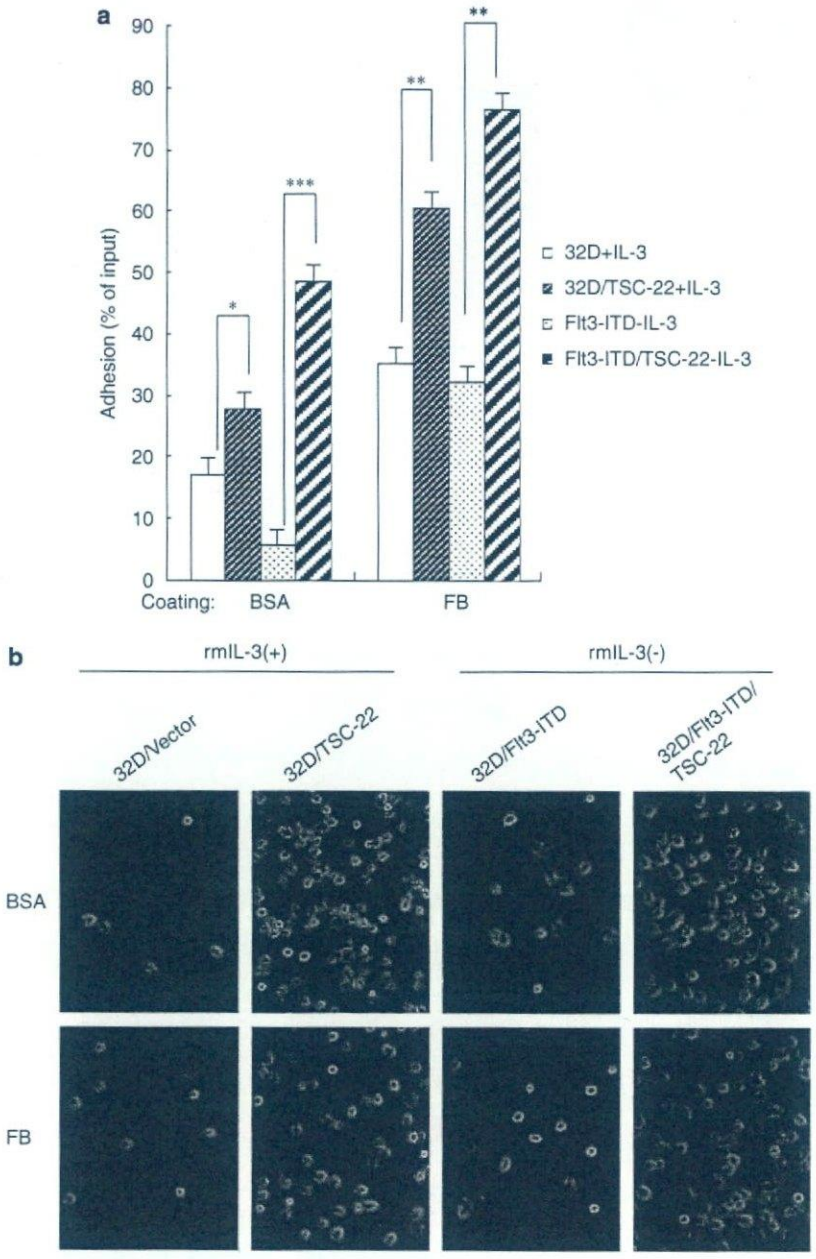

Figure 4 Forced expression of TSC-22 induced adhesion of 32D cells to BSA and FB. 32D and Flt3-ITD-transduced 32D cells infected TSC-22 or vector control viruses were seeded at a density of 2×10^5 cell/ml on 96-well plates coated with BSA or FB for 2 h at 37°C. After washing three times, the percentage of adherent cells was analyzed by Micro Lumat Plus luminometer (**a**) or by microscope (×100) (**b**). The statistical significance of differences between transduced cells and control cells is indicated by asterisks, $***P<0.001$, $**P<0.01$, $*P<0.05$. BSA, bovine serum albumin; FB, Fibrinogen.

showed stronger growth arrest as compared with U937 control cells (Figure 5a). Morphological analysis showed that TSC-22-transduced U937 cells treated with PMA differentiated more efficiently into mature monocytes, the characteristic phenotypes of which were cell spreading, reduced nucleus-to-cytoplasm ratios and appearance of vacuoles (Figure 5b). In accordance with morphological changes, flow cytometry analysis demonstrated that the mean fluorescence intensity (MFI) of CD11b, CD14, CD80 and HLA-DR dramatically increased in TSC-22-expressing U937 cells compared to control U937 cells after PMA treatment, suggesting that differentiation into mature monocytes was efficiently induced in TSC-22-transduced U937 cells (Figure 5c). We also observed similar effects of TSC-22 on Vit.D3-induced differentiation of U937 (Figure 5c).

To further confirm the effect of TSC-22 on the monocytic differentiation of leukemia cells, another human leukemia cell line HL-60 was utilized. As was the case for U937 cells, fluorescence-activated cell sorting analysis showed that higher MFI of CD11b was observed in TSC-22-transduced HL-60 cells as compared with control HL-60 cells in response to either PMA or Vit.D3 (Figure 5d). Collectively, these data suggested that forced expression of TSC-22 played a role in monocytic

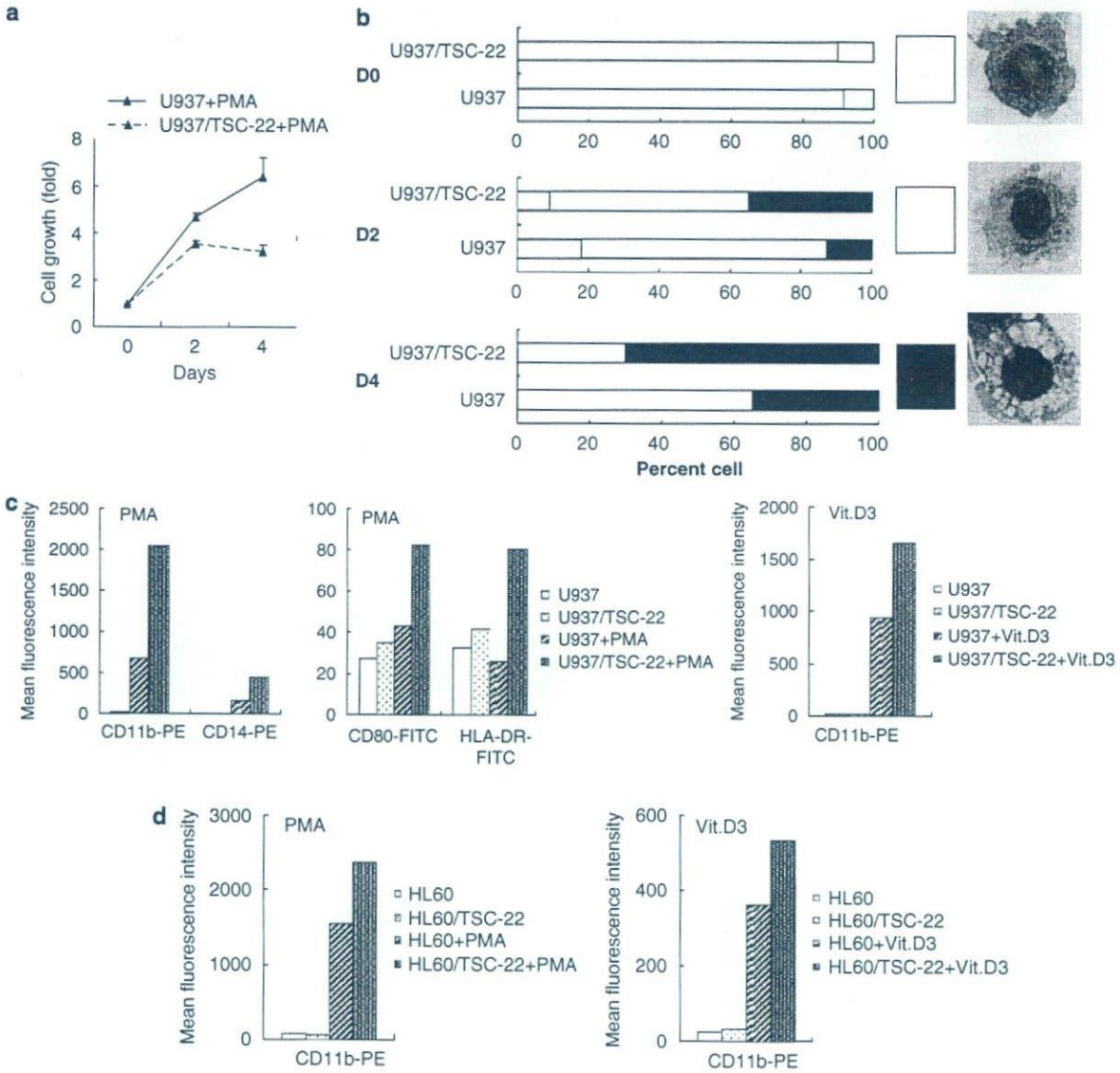

Figure 5 Forced expression of TSC-22 promoted PMA- and Vit.D3-induced monocytic differentiation of human leukemia cell lines. (**a**) Growth inhibition of U937 transfectants with PMA treatment. U937 transfectants were treated with PMA and viable cells of triplicate cultures were quantitated as described previously. (**b**) Differentiation of U937 transfectants with PMA treatment. TSC-22-transduced or control U937 cells were treated with PMA. After 2 or 4 days, cells were stained with May-Grunwald-Giemsa and morphologically analyzed by light microscopy. Cells were grouped into three categories: undifferentiated cells, moderately differentiated cells and terminally differentiated cells. Each photograph on the right column shows typical findings. The percentage of PMA-treated cells under each differentiation stage is shown. (**c**) Surface expression of monocytic markers on U937 transfectants. TSC-22-transduced or control U937 cells were stimulated with PMA or Vit.D3 for 48 h. The surface expression of CD11b, CD14, CD80 and HLA-DR in the cells was evaluated in terms of MFI by flow cytometer. (**d**) Surface expression of monocytic markers on HL-60 transfectants. TSC-22-transduced or control HL-60 cells were stimulated with PMA or Vit.D3 for 48 h. The surface expression of CD11b was evaluated by flow cytometer. HLA-DR, human leukocyte antigen-DR; MFI, mean fluorescence intensity; TSC-22, TGF-β-stimulated clone-22.

differentiation of several leukemia cells. Therefore, TSC-22 appears to have the potential to suppress the growth of several leukemia cells, in part by promoting differentiation into monocytes.

Discussion

Leukemia is caused by multiple gene alterations, including chromosomal translocations, deletions and point mutations. Among them, constitutive activation of a tyrosine kinase receptor Flt3 is the most common mutation found in 30–40% of patients with AML as well as in some patients with myelodysplastic syndromes. There are two types of Flt3 mutations, Flt3-ITD and Flt3-TKD. Overexpression of the WT Flt3 frequently associated with autonomous expression of Flt3 ligand is also found in leukemic patients. These facts indicate that Flt3 activation is pivotal in leukemogenesis in a large population of patients with AML. Both Flt3-ITD and Flt3-TKD constitutively stimulate the downstream signaling pathways;

however, only Flt3-ITD was found to be associated with poor prognosis.[8,12,13,16,20–23]

In the present study, we confirmed that Flt3-ITD was more potent than Flt3-D835V in inducing cell transformation by *in vivo* experiments where Ba/F3 cells expressing Flt3-ITD or Flt3-D835V were transplanted into syngeneic recipient mice. To clarify why Flt3-ITD is more oncogenic than Flt3-TKD, we compared the gene expression profiles of Ba/F3 cells expressing Flt3-ITD and Flt3-D835V. Among the genes upregulated or downregulated by Flt3-D835V as compared with Flt3-ITD, we focused on one of the upregulated genes, TSC-22, a potential tumor suppressor originally identified as a TGF-β-induced gene. Indeed, experiments using an Flt3 inhibitor and Flt3 siRNA confirmed that both expression and kinase activity of Flt3-TKD are required for upregulation of TSC-22. Several studies demonstrated that high expression of TSC-22 inhibited the growth or induced the differentiation of a variety of human tumor cell lines, such as gastric carcinoma cells,[36] breast cancer cells,[32] salivary gland cancer cells,[29,37,38] brain tumors[46] and prostate cancer cells.[47] The findings that anticancer drugs increased or carcinogens decreased the expression of TSC-22 support the concept that TSC-22 can be a key molecule in cancer therapy. TSC-22 expression was also enhanced by various cytokines and growth factors.[26–33] Further study is now under way to determine in which part of signaling pathways TSC-22 integrates. TSC-22 mRNA is expressed in various hematopoietic cell lines as well as bone marrow-derived cells, including macrophages, mast cells and dendritic cells (data not shown). While TSC-22 expression significantly inhibited the growth of several cell lines, including 32D, WEHI and U937, it profoundly inhibited the growth of Flt3-ITD-transduced 32D cells (Figure 3b). Expression of TSC-22 in Ba/F3 cells only weakly inhibited the growth and did not significantly improve the prognosis of Balb/c mice inoculated with Flt3-ITD-transduced Ba/F3 cells (data not shown). This is probably because the endogenous expression level of TSC-22 in Ba/F3 cells is much higher than those in other cell lines (data not shown). Therefore, we used 32D cells in both *in vitro* and *in vivo* experiments that express much less amount of TSC-22. A dominant-negative form of TSC-22 accelerated the growth of 32D cells, which is consistent with the growth suppressive effects of TSC-22 on leukemic cells. In addition, expression of TSC-22 in Flt3-ITD-transduced 32D cells seemed to improve the prognosis of C3H/HeJ mice inoculated with Flt3-ITD-transduced 32D cells. Thus, although we still do not know if the difference in clinical outcomes is relevant to the differing expression levels of TSC-22 downstream of Flt3-ITD and Flt3-TKD, the increased expression of TSC-22 may explain at least in part the attenuated growth of Flt3-TKD-expressing cells when compared to Flt3-ITD-expressing cells. According to recent reports, activation of STAT5, mitogen-activated protein kinase (MAPK) and protein kinase B(Akt) and repression of the myeloid transcription factors CCAAT/enhancer binding protein α (EβPα) and PU.1 are relevant to potent transforming abilities of Flt3-ITD-bearing cells.[18,24,25,48] However the activation of STAT5, MAPK and Akt was not affected by enforced expression of TSC-22 (data not shown), suggesting that TSC-22 is rather downstream but not upstream of these signaling molecules. Further investigation is required where and how TSC-22 integrates in the signal transduction pathway. To fully evaluate the impact of TSC-22 on leukemogenesis, experiments involving bone marrow transplantation using TSC-22 knock out mice will be useful.

In general, the suppression of growth is associated with the induction of apoptosis or cell-cycle arrest. In fact, TSC-22 induces the apoptosis of several cancer cells, as reported by Ohta *et al.*[36] and Uchida *et al.*[49] However, neither apoptosis nor cell-cycle arrest was significantly induced in TSC-22-transduced leukemia cells (data not shown). Instead, we found that monocytic differentiation of several leukemia cells was accelerated by the forced expression of TSC-22. This effect was more evident when differentiation-inducing reagents were given (Figures 5c and d). On the other hand, G-CSF-induced granulocytic differentiation of 32D cells was not enhanced by TSC-22 expression.

A differentiation block is one of the two major causes of leukemogenesis, acting in concert with progressive proliferation or inhibition of apoptosis. Thus, TSC-22 may exert growth-suppressive effects on leukemia cells in part through the acceleration of monocytic differentiation. Although Choi *et al.*[50] reported that TSC-22-induced erythroid differentiation of K562 cells by enhancing TGF-β signaling, the differentiation was not induced by cooperation with TGF-β signaling in the TSC-22-transduced leukemia cells we used. In acute promyelocytic leukemia (APL), all-*trans* retinoic acid (ATRA) is a potent inducer of differentiation in APL cells. Moreover, combinatorial use of ATRA and G/granulocyte macrophage-CSF promoted myelomonocytic differentiation, as reported by Glasow *et al.*[51] Our data, together with recent findings, suggest that combination of chemical compounds that increase TSC-22 expression and differentiation-inducing drugs will be attractive as a new therapy for leukemia. TSC-22 is considered to be a transcriptional regulator because of its leucine zipper-like structure; however, the precise mechanism by which TSC-22 functions in the differentiation of leukemia cells remains to be elucidated.

In conclusion, the increased expression of TSC-22 downstream of Flt3-D835V was not observed downstream of Flt3-ITD. Forced expression of TSC-22 suppresses the growth and promotes the monocytic differentiation of several leukemia cells, in particular, in combination with differentiation-inducing reagents. TSC-22 appears promising in developing more effective therapy for leukemia.

Acknowledgements

We thank Dr Hitoshi Kawamata for providing plasmid pEGFP-TSC-22-LZ. We thank Dr Naoko Watanabe, Dr Yoshinori Yamanishi, Dr Kumi Izawa and Dr Yukinori Minoshima for valuable discussions, Fumi Shibata, Miyuki Ito and Ai Hishiya for excellent technical assistance. We also thank R&D Systems for cytokines. This work was supported in part by Grants-in-Aid from the Ministry of Education, Science, Technology, Sports, and Culture in Japan.

References

1 Matthews W, Jordan CT, Wiegand GW, Pardoll D, Lemischka IR. A receptor tyrosine kinase specific to hematopoietic stem and progenitor cell-enriched populations. *Cell* 1991; **65**: 1143–1152.
2 Rosnet O, Marchetto S, deLapeyriere O, Birnbaum D. *Oncogene* 1991; **6**: 1641–1650.
3 Small D, Levenstein M, Kim E, Carow C, Amin S, Rockwell P *et al.* STK-1, the human homolog of Flk-2/Flt3, is selectively expressed in CD34+ human bone marrow cells and is involved in the proliferation of early progenitor/stem cells. *Proc Natl Acad Sci USA* 1994; **91**: 459–463.
4 Rosnet O, Buhring HJ, Marchetto S, Rappold I, Lavagna C, Sainty D *et al.* Human FLT3/FLK2 receptor tyrosine kinase is expressed at the surface of normal and malignant hematopoietic cells. *Leukemia* 1996; **10**: 238–248.
5 Mackarehtschian K, Hardin JD, Moore KA, Boast S, Goff SP, Lemischka IR. Targeted disruption of the flk2/flt3 gene leads to

deficiencies in primitive hematopoietic progenitors. *Immunity* 1995; **3**: 147–161.
6 Birg F, Courcoul M, Rosnet O, Bardin F, Pebusque MJ, Marchetto S *et al.* Expression of the FMS/KIT-like gene FLT3 in human acute leukemias of the myeloid and lymphoid lineages. *Blood* 1992; **80**: 2584–2593.
7 Carow CE, Levenstein M, Kaufmann SH, Chen J, Amin S, Rockwell P *et al.* Expression of the hematopoietic growth factor receptor FLT3 (STK-1/Flk2) in human leukemias. *Blood* 1996; **87**: 1089–1096.
8 Nakao M, Yokota S, Iwai T, Kaneko H, Horiike S, Kashima K *et al.* Internal tandem duplication of the Flt3 gene found in acute myeloid leukemia. *Leukemia* 1996; **10**: 1911–1918.
9 Kiyoi H, Towatari M, Yokota S, Hamaguchi M, Ohno R, Saito H *et al.* Internal tandem duplication of the FLT3 gene is a novel modality of elongation mutation which causes constitutive activation of the product. *Leukemia* 1998; **12**: 1333–1337.
10 Meshinchi S, Woods WG, Stirewalt DL, Sweetser DA, Buckley JD, Tjoa TK *et al.* Prevalence and prognostic significance of Flt3 internal tandem duplication in pediatric acute myeloid leukemia. *Blood* 2001; **97**: 89–94.
11 Stirewalt DL, Kopecky KJ, Meshinchi S, Appelbaum FR, Slovak ML, Willman CL *et al.* FLT3, RAS and TP53 mutations in elderly patients with acute myeloid leukemia. *Blood* 2001; **97**: 3589–3595.
12 Schnittger S, Schoch C, Dugas M, Kern W, Staib P, Wuchter C *et al.* Analysis of FLT3 length mutations in 1003 patients with acute myeloid leukemia: correlation to cytogenetics, FAB subtype, and prognosis in the AMLCG study and usefulness as a marker for the detection of minimal residual disease. *Blood* 2002; **100**: 59–66.
13 Thiede C, Steudel C, Mohr B, Schaich M, Schakel U, Platzbecker U *et al.* Analysis of FLT3-activating mutations in 979 patients with acute myelogenous leukemia: association with FAB subtypes and identification of subgroups with poor prognosis. *Blood* 2002; **99**: 4326–4335.
14 Yamamoto Y, Kiyoi H, Nakano Y, Suzuki R, Kodera Y, Miyawaki S *et al.* Activating mutation of D835 within the activation loop of FLT3 in human hematologic malignancies. *Blood* 2001; **97**: 2434–2439.
15 Abu-Duhier FM, Goodeve AC, Wilson GA, Care RS, Peake IR, Reilly JT. Identification of novel FLT3 Asp835 mutations in adult acute myeloid leukaemia. *Br J Haematol* 2001; **113**: 983–988.
16 Kottaridis PD, Gale RE, Frew ME, Harrison G, Langabeer SE, Belton AA *et al.* The presence of a FLT3 internal tandem duplication in pa-tients with acute myeloid leukemia (AML) addsimportant prognostic information to cytogeneticrisk group and response to the first cycle of che-motherapy: analysis of 854 patients from theUnited Kingdom Medical Research Council AML10 and 12 trials. *Blood* 2001; **98**: 1752–1759.
17 Hayakawa F, Towatari M, Kiyoi H, Tanimoto M, Kitamura T, Saito H *et al.* Tandem-duplicated Flt3 constitutively activates STAT5 and MAP kinase and introduces autonomous cell growth in IL-3-dependent cell lines. *Oncogene* 2000; **19**: 624–631.
18 Mizuki M, Fenski R, Halfter H, Matsumura I, Schmidt R, Muller C *et al.* Flt3 mutations from patients with acute myeloid leukemia induce transformation of 32D cells mediated by the Ras and STAT5 pathways. *Blood* 2000; **96**: 3907–3914.
19 Fenski R, Flesch K, Serve S, Mizuki M, Oelmann E, Kratz-Albers K *et al.* Constitutive activation of FLT3 in acute myeloid leukaemia and its consequences for growth of 32D cells. *Br J Haematol* 2000; **108**: 322–330.
20 Stirewalt DL, Radich JP. The role of FLT3 in haematopoietic malignancies. *Nat Rev Cancer* 2003; **3**: 650–665.
21 Shih LY, Huang CF, Wu JH, Lin TL, Dunn P, Wang PN *et al.* Internal tandem duplication of FLT3 in relapsed acute myeloid leukemia: a comparative analysis of bone marrow samples from 108 adult patients at diagnosis and relapse. *Blood* 2002; **100**: 2387–2392.
22 Moreno I, Martin G, Bolufer P, Barragan E, Rueda E, Roman J *et al.* Incidence and prognostic value of FLT3 internal tandem duplication and D835 mutations in acute myeloid leukemia. *Haematologica* 2003; **88**: 19–24.
23 Levis M, Small D. FLT3: ITDoes matter in leukemia. *Leukemia* 2003; **17**: 1738–1752.
24 Spiekermann K, Bagrintseva K, Schwab R, Schmieja K, Hiddemann W. Overexpression and constitutive activation of FLT3 induces STAT5 activation in primary acute myeloid leukemia blast cells. *Clin Cancer Res* 2003; **9**: 2140–2150.
25 Choudhary C, Schwable J, Brandts C, Tickenbrock L, Sargin B, Kindler T *et al.* AML-associated Flt3 kinase domain mutations show signal transduction differences compared with Flt3 ITD mutations. *Blood* 2005; **106**: 265–273.
26 Shibanuma M, Kuroki T, Nose K. Isolation of a gene encoding a putative leucine zipper structure that is induced by transforming growth factor beta 1 and other growth factors. *J Biol Chem* 1992; **267**: 10219–10224.
27 Ohta S, Shimekake Y, Nagata K. Molecular cloning and characterization of a transcription factor for the C-type natriuretic peptide gene promoter. *Eur J Biochem* 1996; **242**: 460–466.
28 Jay P, Ji JW, Marsollier C, Taviaux S, Berge-Lefranc JL, Berta P. Cloning of the human homologue of the TGF beta-stimulated clone 22 gene. *Biochem Biophys Res Commun* 1996; **222**: 821–826.
29 Kawamata H, Nakashiro K, Uchida D, Hino S, Omotehara F, Yoshida H *et al.* Induction of TSC-22 by treatment with a new anti-cancer drug, vesnarinone, in a human salivary gland cancer cell. *Br J Cancer* 1998; **77**: 71–78.
30 Hamil KG, Hall SH. Cloning of rat Sertoli cell follicle-stimulating hormone primary response complementary deoxyribonucleic acid: regulation of TSC-22 gene expression. *Endocrinology* 1994; **134**: 1205–1212.
31 Kawa-uchi T, Nifuji A, Mataga N, Olson EN, Bonaventure J, Shinomiya K *et al.* Fibroblast growth factor downregulates expression of a basic helix-loop-helix-type transcription factor, scleraxis, in a chondrocyte-like cell line, TC6. *J Cell Biochem* 1998; **70**: 468–477.
32 Kester HA, van der Leede BM, van der Saag PT, van der Burg B. Novel progesterone target genes identified by an improved differential display technique suggest that progestin-induced growth inhibition of breast cancer cells coincides with enhancement of differentiation. *J Biol Chem* 1997; **272**: 16637–16643.
33 Trenkle T, Welsh J, Jung B, Mathieu-Daude F, McClelland M. Non-stoichiometric reduced complexity probes for cDNA arrays. *Nucleic Acids Res* 1998; **26**: 3883–3891.
34 Dohrmann CE, Belaoussoff M, Raftery LA. Dynamic expression of TSC-22 at sites of epithelial-mesenchymal interactions during mouse development. *Mech Dev* 1999; **84**: 147–151.
35 Kester HA, Ward-van Oostwaard TM, Goumans MJ, van Rooijen MA, van Der Saag PT, van Der Burg B *et al.* Expression of TGF-beta stimulated clone-22 (TSC-22) in mouse development and TGF-beta signalling. *Dev Dyn* 2000; **218**: 563–572.
36 Ohta S, Yanagihara K, Nagata K. Mechanism of apoptotic cell death of human gastric carcinoma cells mediated by transforming growth factor beta. *Biochem J* 1997; **324**: 777–782.
37 Nakashiro K, Kawamata H, Hino S, Uchida D, Miwa Y, Hamano H *et al.* Down-regulation of TSC-22 (transforming growth factor beta-stimulated clone 22) markedly enhances the growth of a human salivary gland cancer cell line *in vitro* and *in vivo*. *Cancer Res* 1998; **58**: 549–555.
38 Hino S, Kawamata H, Uchida D, Omotehara F, Miwa Y, Begum NM *et al.* Nuclear translocation of TSC-22 (TGF-beta-stimulated clone-22) concomitant with apoptosis: TSC-22 as a putative transcriptional regulator. *Biochem Biophys Res Commun* 2000; **278**: 659–664.
39 Murata K, Kumagai H, Kawashima T, Tamitsu K, Irie M, Nakajima H *et al.* Selective cytotoxic mechanism of GTP-14564, a novel tyrosine kinase inhibitor in leukemia cells expressing a constitutively active Fms-like tyrosine kinase 3 (FLT3). *J Biol Chem* 2003; **278**: 32892–32898.
40 Kitamura T, Koshino Y, Shibata F, Oki T, Nakajima H, Nosaka T *et al.* Retrovirus-mediated gene transfer and expression cloning powerful tools in functional genomics. *Exp Hematol* 2003; **31**: 1007–1014.
41 Oki T, Kitaura J, Eto K, Lu Y, Maeda-Yamamoto M, Inagaki N *et al.* Integrin alphaIIbbeta3 induces the adhesion and activation of mast cells through interaction with fibrinogen. *J Immunol* 2006; **76**: 52–60.
42 Weisberg E, Boulton C, Kelly LM, Manley P, Fabbro D, Meyer T *et al.* Inhibition of mutant FLT3 receptors in leukemia cells by the

small molecule tyrosine kinase inhibitor PKC412. *Cancer Cell* 2002; **1**: 433–443.
43 Walters DK, Stoffregen EP, Heinrich MC, Deininger MW, Druker BJ. RNAi-induced down-regulation of FLT3 expression in AML cell lines increases sensitivity to MLN518. *Blood* 2005; **105**: 2952–2954.
44 Kester HA, Blanchetot C, den Hertog J, van der Saag PT, van der Burg B. Transforming growth factor-beta-stimulated clone-22 is a member of a family of leucine zipper proteins that can homo- and heterodimerize and has transcriptional repressor activity. *J Biol Chem* 1999; **274**: 27439–27447.
45 Zheng R, Friedman AD, Small D. Targeted inhibition of FLT3 overcomes the block to myeloid differentiation in 32Dcl3 cells caused by expression of FLT3/ITD mutations. *Blood* 2002; **100**: 4154–4161.
46 Shostak KO, Dmitrenko VV, Garifulin OM, Rozumenko VD, Khomenko OV, Zozulya YA *et al*. Downregulation of putative tumor suppressor gene TSC-22 in human brain tumors. *J Surg Oncol* 2003; **82**: 57–64.
47 Rentsch CA, Cecchini MG, Schwaninger R, Germann M, Markwalder R, Heller M *et al*. Differential expression of TGF beta-stimulated clone 22 in normal prostate and prostate cancer. *Int J Cancer* 2006; **118**: 899–906.
48 Mizuki M, Schwable J, Steur C, Choudhary C, Agrawal S, Sargin B *et al*. Suppression of myeloid transcription factors and induction of STAT response genes by AML-specific Flt3 mutations. *Blood* 2003; **101**: 3164–3173.
49 Uchida D, Kawamata H, Omotehara F, Miwa Y, Hino S, Begum NM *et al*. Over-expression of TSC-22 (TGF-beta stimulated clone-22) markedly enhances 5-fluorouracil-induced apoptosis in a human salivary gland cancer cell line. *Lab Invest* 2000; **80**: 955–963.
50 Choi SJ, Moon JH, Ahn YW, Ahn JH, Kim DU, Han TH. Tsc-22 enhances TGF-beta signaling by associating with Smad4 and induces erythroid cell differentiation. *Mol Cell Biochem* 2005; **271**: 23–28.
51 Glasow A, Prodromou N, Xu K, von Lindern M, Zelent A. Retinoids and myelomonocytic growth factors cooperatively activate RARA and induce human myeloid leukemia cell differentiation via MAP kinase pathways. *Blood* 2005; **105**: 341–349.